P-04-126

Forsmark site investigation

Bedrock mapping U-Pb, $^{40}Ar/^{39}Ar$ and (U-Th)/He geochronology

Page L, Hermansson T, Söderlund P
Department of Geology, University of Lund

Andersson J, Stephens M B
Geological Survey of Sweden, Uppsala

May 2004

Svensk Kärnbränslehantering AB
Swedish Nuclear Fuel
and Waste Management Co
Box 5864
SE-102 40 Stockholm Sweden
Tel 08-459 84 00
+46 8 459 84 00
Fax 08-661 57 19
+46 8 661 57 19

ISSN 1651-4416
SKB P-04-126

Forsmark site investigation

Bedrock mapping U-Pb, $^{40}Ar/^{39}Ar$ and (U-Th)/He geochronology

Page L, Hermansson T, Söderlund P
Department of Geology, University of Lund

Andersson J, Stephens M B
Geological Survey of Sweden, Uppsala

May 2004

Keywords: Forsmark, Geochronology, Thermochronology, Zircon, Titanite, Hornblende, Biotite, Apatite, TIMS, NORDSIM, AP PF 400-02-11, Field note no Forsmark 22 .

Abstract

The present study aims, with the help of different geochronological systems, to reconstruct the temperature-time history of the bedrock at the Forsmark site, from the time of crystallization of the intrusive rocks through to the time when the rocks were uplifted through the c 70–60°C isotherm. The geochronological analytical programme has involved the analysis of different minerals in different isotopic systems with different blocking temperatures. In order of decreasing blocking temperature, these systems are U-Pb zircon (SIMS and TIMS techniques), U-Pb titanite (TIMS technique), $^{40}Ar/^{39}Ar$ hornblende, $^{40}Ar/^{39}Ar$ biotite, and (U-Th)/He apatite. 31 age determinations have been completed. The 25 samples analysed come from different groups of meta-intrusive rocks at the Forsmark site, from contrasting ductile structural domains, and from different bedrock blocks between regionally important deformation zones (Forsmark, Eckarfjärden, Singö).

Bearing in mind the analytical errors, an older suite of calc-alkaline, meta-intrusive rocks, with tonalitic to granodioritic and gabbroic compositions (Group B), have yielded crystallisation ages in the time range 1887 to 1880 Ma. The metagranite in the candidate area (Group B) has yielded a younger age of 1865±3.4 Ma and a minor intrusion with granodioritic composition (Group C), which belongs to a younger suite of calc-alkaline rocks, has given a similar age (1864±3 Ma). A sample from a suite of granite dykes (Group D) that are strongly discordant to the intense tectonic banding in the rocks along the coast, to the northeast of the candidate area, has yielded a crystallisation age of 1851±5 Ma. The intense ductile deformation in the coastal area is constrained to the time interval 1868 to 1846 Ma. Ductile deformation along more discrete ductile deformation zones at the Forsmark site, which locally affected the Group D rocks, is inferred to have occurred after 1856 Ma.

Cooling below the 700–550°C isotherm occurred in the time interval 1848–1840 Ma and below the c 500°C isotherm in the time interval 1834–1793 Ma. An apparent difference has been detected in the cooling ages below the 500°C isotherm, in surface samples from the different ductile, structural domains. Cooling below the c 300°C isotherm occurred in the time interval 1704–1635 Ma and below the 70–60°C isotherm in the time interval c 630–250 Ma. There also appear to be differences in the cooling ages below these two isotherms in surface samples from different bedrock blocks. Furthermore, the cooling ages beneath these two isotherms decrease, as expected, with depth in borehole KFM01A. The borehole data have also revealed a possible exhumation event at c 300–250 Ma. More data from both surface and borehole samples are required to understand better the important geological implications of these spatial variations.

Sammanfattning

Syftet med denna studie är, att med hjälp av olika geokronologiska metoder rekonstruera den magmatiska utvecklingen samt deformations- och avkylningshistorien i Forsmarksområdets berggrund. Den dokumenterade delen av händelseförloppet började med kristallisationen av de intrusiva bergarterna och pågick under den tid då bergarterna lyftes upp genom den nivå i jordskorpan som håller en temperatur på 70–60º C Det geokronologiska programmet omfattade analys av olika mineral i flera isotopsystem med skilda stängningstemperaturer. I ordningsföljd efter minskande stängningstemperatur är de isotopiska systemen; U-Pb i zircon (SIMS- och TIMS-metoderna), U-Pb i titanit (TIMS), $^{40}Ar/^{39}Ar$ i hornblände, $^{40}Ar/^{39}Ar$ i biotit och (U-Th)/He i apatit. Totalt har 31 åldersbestämningar utförts. De 25 analyserade proverna kommer från olika metaintrusiva bergartsgrupper i Forsmarksområdet, från domäner med sinsemellan starkt varierande plastisk deformation och från olika berggrundsblock som ligger mellan regionalt betydelsefulla deformationszoner (Forsmarks-, Eckarfjärden- och Singözonen).

En äldre svit av kalkalkalina metaintrusiva bergarter, med tonalitisk till granodioritisk och gabbroisk sammansättning (grupp B), gav en kristallisationsålder (med reservation för analysfel) i tidsintervallet 1887–1880 miljoner år. Metagraniten i kandidatområdet (grupp B) visade sig ha en lägre ålder, 1865±3,4 miljoner år, och en mindre intrusion med granodioritisk sammansättning (grupp C), som tillhör en yngre svit av kalkalkalina bergarter, gav en liknande ålder (1864±3 milj. år). Grupp D omfattar en svit av granitgångar som är starkt diskordanta mot den intensiva tektoniska bandningen i bergarterna längs kusten, nordost om kandidatområdet. Ett prov från granitgångarna gav en kristallisationsålder på 1851±5 miljoner år. Den starka plastiska deformationen i kustområdet är begränsad i tiden till intervallet 1868–1846 miljoner år sedan. Plastisk deformation längs mer begränsade zoner vid Forsmarksområdet som påverkar Grupp D bergarterna anses ha pågått senare än för 1856 miljoner år sedan.

Avkylning under nivån för 700–550º C ägde rum för 1848–1840 miljoner år sedan och under 500º C-nivån för 1834–1793 miljoner år sedan. Påtagliga skillnader i avkylningsålder under 500º C-nivån har upptäckts mellan ytliga bergartsprover från de olika plastiska, strukturella domänerna. Avkylning under 300º C-nivån skedde för 1704–1639 miljoner år sedan och under 70–60º C-nivån för 630–250 miljoner år sedan. Det tycks också finnas skillnader i avkylningsålder under de båda senare nivåerna i prover från olika bergartsblock. Dessutom minskar avkylningsåldern under de båda nivåerna som väntat mot djupet i borrhål KFM01A. Data från borrhålet har också avslöjat en möjlig uppåtrörelse i berggrunden för 300–250 miljoner år sedan. Det behövs ytterligare information, både från markytan och från borrhål, för att bättre förstå den geologiskt viktiga innebörden av de tredimensionella variationerna.

Contents

1 Introduction

Geological mapping of the crystalline bedrock forms one of the major surface activities performed within the initial site investigation programme at the Forsmark site. The work follows the directives in the steering document for the activity that is entitled "Bedrock mapping at Forsmark, 2002–2003" (AP PF 400-02-11) and has involved several subprojects. These subprojects have been carried out in accordance with the method description for bedrock mapping (SKB MD 132.001).

The prime aim of the bedrock-mapping activity is to present a new, detailed geological map of the crystalline bedrock in the candidate area at Forsmark and its surroundings, at the scale 1:10 000. The area selected for mapping is shown in Figure 1-1. The first version of this map (Version 1.1), which was based on all the geological and geophysical information available at the end of April 2003, was presented earlier /SKB GIS database under field note no 22/. The second and final version of the bedrock geological map of the Forsmark site (Version 1.2), based on all the information available at the end of April 2004, has recently been delivered to SKB /SKB GIS database under field note no 22/. A version of this map, suitable for presentation in the context of this report, is shown in Figure 1-2.

The bedrock-mapping project has been organised into several distinct working phases and has involved execution of activities during two time stages, 2002 and 2003. Many of the results of the various subprojects have already been presented in several reports /Bergman et al, 2004; Isaksson, 2003; Isaksson et al, 2004a; Mattsson et al, 2003; Stephens et al, 2003a, 2003b/. Furthermore, use has been made of the results of work in complementary projects, steered by separate activity documents /see, for example, Isaksson et al, 2004b/. This report presents the results of the geochronological work that has been completed within the context of the bedrock-mapping project.

Felsic to intermediate metavolcanic rocks (Group A) and three groups of meta-intrusive rocks (Groups B, C and D) have been recognised /Stephens et al, 2003b/ in connection with the bedrock-mapping activities at Forsmark (Figure 1-2 and Table 1-1). The intrusive rocks that belong to Group B and to Groups C and D, respectively, form two separate calc-alkaline suites of igneous rocks.

The calc-alkaline intrusive rocks in Group B, as well as the supracrustal rocks in Group A, were affected by penetrative ductile deformation under amphibolite-facies metamorphic conditions, prior to intrusion of the younger suite of calc-alkaline intrusive rocks that belong to Groups C and D (Table 1-1). The intrusive rocks included in Groups C and D were also affected by ductile deformation, probably under lower amphibolite- and greenschist-facies metamorphic conditions. However, pervasive ductile deformation at the Forsmark site was completed prior to intrusion of the granites and at least some of the pegmatites included in the Group D rocks.

The Forsmark site can be divided into contrasting structural domains /Stephens et al. 2003b/. SL-tectonites and an inferred higher degree of ductile deformation characterise the areas, for example, to the southwest and to the northeast of the candidate area (Figure 1-2). By contrast, LS-tectonites, folding and an inferred lower degree of ductile deformation characterise, for example, the candidate area (Figure 1-2).

The deformation in the bedrock that accompanied and/or followed intrusion of the Group D rocks was discrete in character and was restricted to high-strain zones, with combined ductile and brittle or solely brittle character (Table 1-1). The most conspicuous regional deformation zones in the area strike in a north-west direction and include the Forsmark, Eckarfjärden and Singö deformation zones (Figure 1-2). These zones divide the bedrock into different structural blocks.

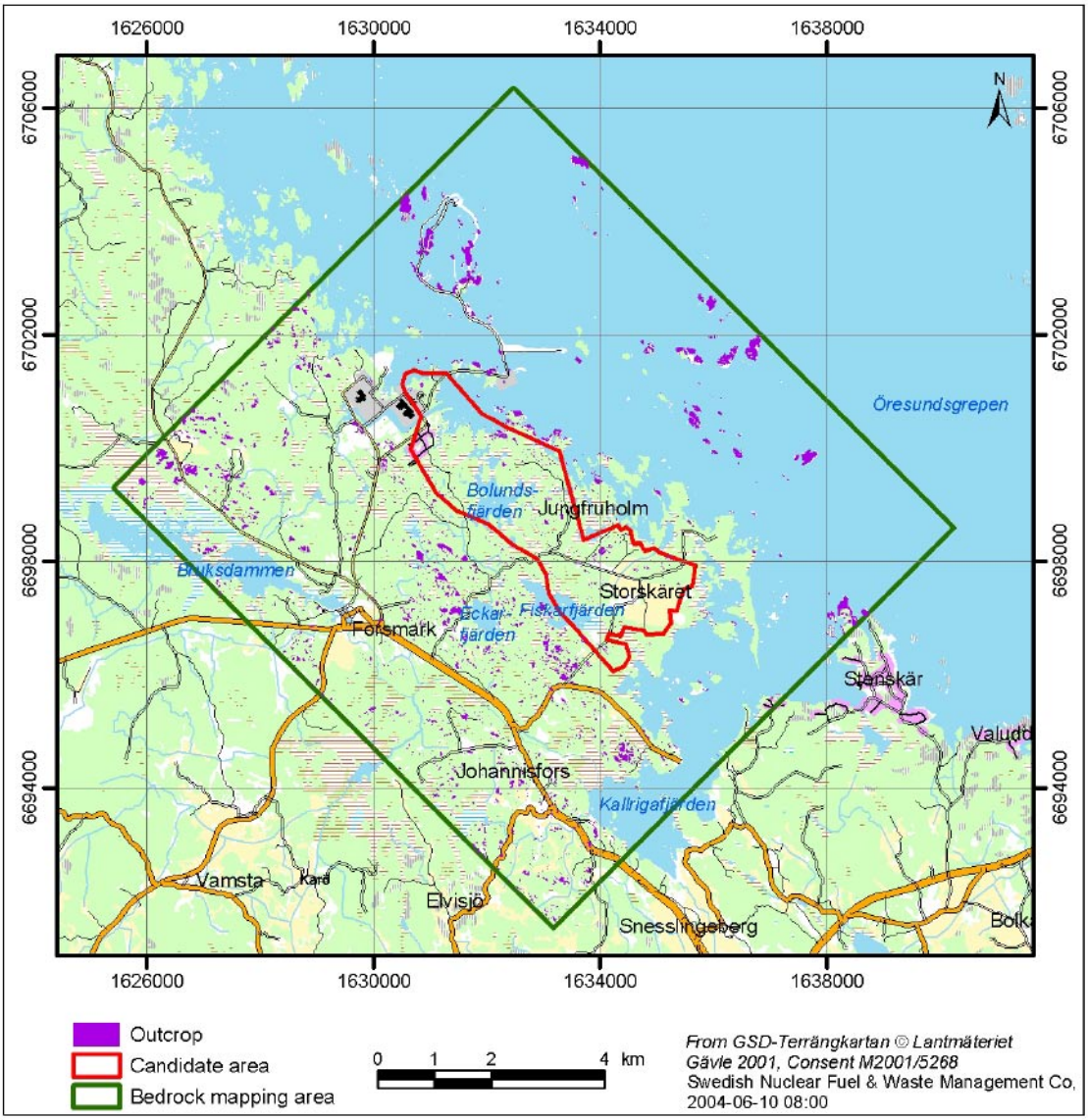

Figure 1-1. *Location of the area selected for bedrock mapping at the Forsmark site.*

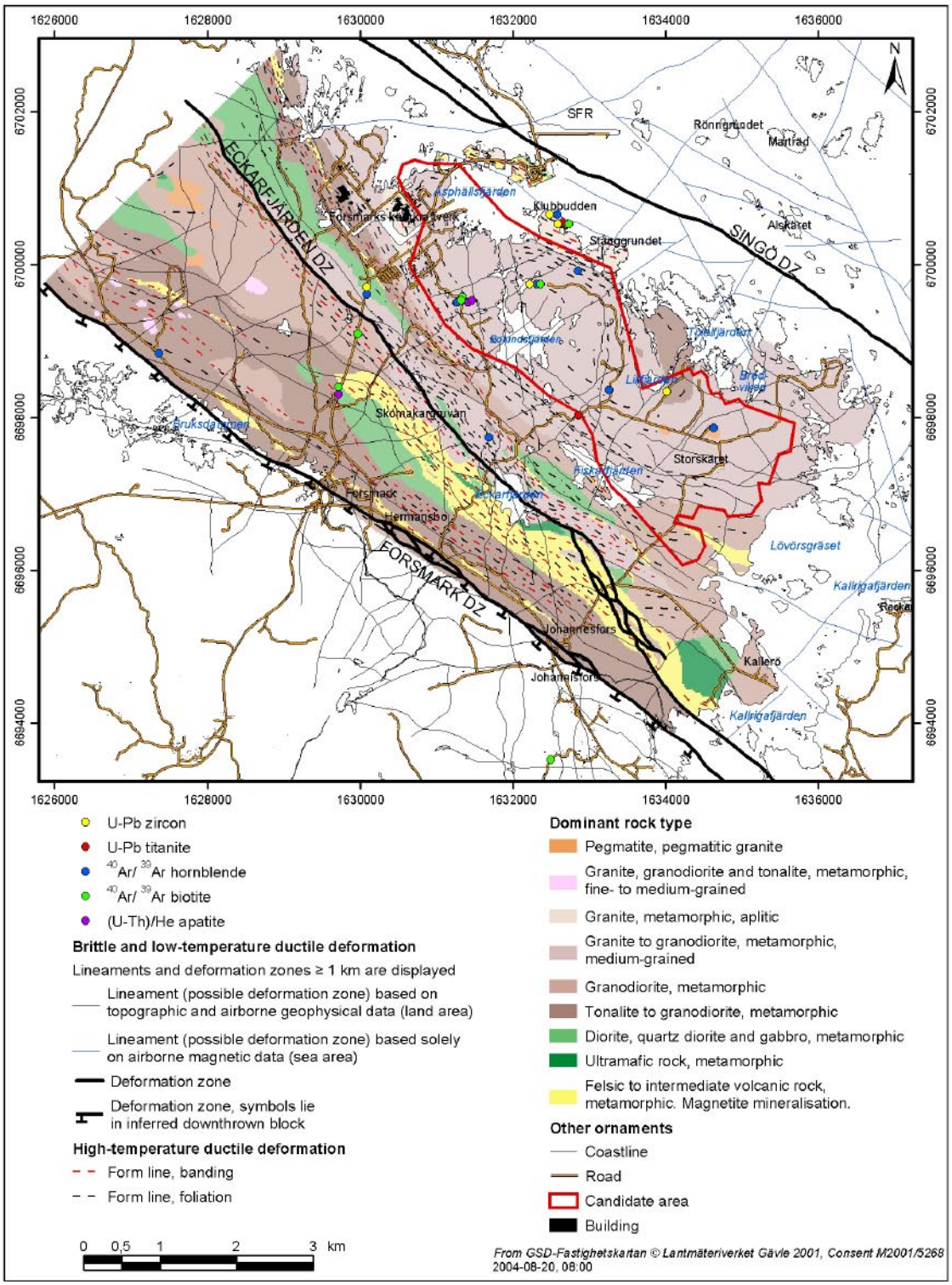

Figure 1-2. *Bedrock geological map of the Forsmark site, based on Version 1.1 /SKB GIS database under field note no 22/, and location of samples selected for geochronological purposes.*

Table 1-1. Major groups of rock at the Forsmark site.

Rock types	
All rocks affected by brittle deformation. The fractures generally cut the boundaries between the different rock types (sealed boundaries).	
Rocks in Group D affected, in part, by ductile deformation and metamorphism.	
Group D	Fine- to medium-grained granite, aplite, pegmatitic granite and pegmatite. Occur as dykes and minor bodies that are commonly discordant to earlier ductile deformation. Variable age relationships with respect to Group C.
Rocks in Group C affected by ductile deformation under lower amphibolite-facies metamorphic conditions.	
Group C	Fine- to medium-grained granodiorite, tonalite and subordinate granite. Occur as lenses and dykes in Groups A and B. Intruded after some ductile deformation in the rocks belonging to Groups A and B.
Rocks in Groups A and B affected by ductile deformation under amphibolite-facies metamorphic conditions.	
Group B	Biotite-bearing granite (to granodiorite) and aplitic granite, both with amphibolite as dyke-like bodies and irregular inclusions.
	Granodiorite and tonalite to granodiorite with amphibolite enclaves.
	Quartz diorite to gabbro, ultramafic rock.
Group A	Volcanic rocks and iron oxide mineralisation. Sulphide mineralisation

2 Objective and Scope

The present study aims, with the help of different geochronological systems, to reconstruct the temperature-time history of the bedrock at the Forsmark site, from crystallization through to the time when the rocks were uplifted through the c 70–60°C isotherm. The geochronological analytical programme has involved the analysis of different minerals in different isotopic systems with different blocking temperatures. In order of decreasing blocking temperature, these systems are U-Pb zircon, U-Pb titanite, $^{40}Ar/^{39}Ar$ hornblende, $^{40}Ar/^{39}Ar$ biotite, and (U-Th)/He apatite. The results are documented in this order in this report.

The geochronological investigations at Forsmark have been subdivided into two principal subprojects that have addressed 1) high-T (>500°C) geochronology and 2) low-T (<500°C) geochronology. Both studies form parts of two Ph.D. projects that are financed partly by the University of Lund and partly by SKB (high-T geochronology, Tobias Hermansson; low-T geochronology, Pia Söderlund).

The prime objective of the high-T geochronology work has been to date the crustal growth and the high-T tectonothermal evolution down to cooling at c 500°C. This subproject has included conventional U-Pb zircon and U-Pb titanite analyses in order to constrain igneous crystallisation ages and the timing of cooling through the temperature interval c 700–550°C. However, due to the complex nature of some of the zircons, it was judged necessary to use the in-situ capability of the NORDSIM instrument at the Swedish Museum of Natural History in Stockholm. With the help of this technique, it is possible to separate igneous crystallisation ages from complications caused by, for example, secondary zircon growth in connection with later metamorphic events. Finally, $^{40}Ar/^{39}Ar$ hornblende analyses were obtained to constrain the regional cooling below 500°C. The zircons, titanites and hornblendes that have been analysed have all been separated from surface samples.

The low-T thermochronology project has aimed to constrain the cooling of the bedrock at the Forsmark site below c 300°C with the help of $^{40}Ar/^{39}Ar$ analyses of biotite and the temperature of uplift through c 70–60°C using (U-Th)/He dating of apatite. Biotite and apatite have been separated and analysed from both surface and drill-core samples.

A complete list of all the samples analysed in this study, in combination with the geochronological method(s) that was used, is presented in Table 2-1. The samples analysed for geochronological purposes are also illustrated on the geological map in Figure 1-2. The assessment of the character of each sample is based on the documented field relationships /Stephens et al, 2003a/ as well as, in most cases, modal and geochemical analyses /Stephens et al, 2003b/. Samples for geochronology were taken from each of the three groups of meta-intrusive rocks (Groups B, C and D), from both types of structural domain, and from the different bedrock blocks between the regionally important deformation zones. The dating of the meta-intrusive rocks also provides a minimum age for the supracrustal rocks at the site (Group A).

Geochronological work has been carried out on 25 samples. Furthermore, different analytical techniques have been used on several of these samples. In total, 31 age determinations have been obtained, which together provide different types of geological information. This report aims to present the results of this geochronological investigation and to provide the geological interpretation of the ages obtained. No attempt is made here to evaluate the broader geological implications of these new geochronological data.

Table 2-1. Samples analysed for geochronological purposes at the Forsmark site and the methods employed.

Sample	Northing in RT 90, 2.5 gon V (metres)	Easting in RT 90, 2.5 gon V (metres)	Rock group	Rock type	Method of dating
PFM000256A	6699088	1629974	B	Metagranite to metagranodiorite	$^{40}Ar/^{39}Ar$ biotite
PFM000718G	6700543	1632654	D	Granite dyke	U-Pb titanite
PFM000875A	6698352	1629723	B	Metatonalite	$^{40}Ar/^{39}Ar$ biotite, (U-Th)/He apatite
PFM001183B	6698019	1632862	B	Amphibolite	U-Pb titanite
PFM001240A	6693523	1632499	B	Metagranodiorite	$^{40}Ar/^{39}Ar$ biotite
PFM002207A	6699740	1632290	B	Metagranite	U-Pb zircon, $^{40}Ar/^{39}Ar$ biotite
PFM002208A	6699743	1632308	B	Amphibolite	$^{40}Ar/^{39}Ar$ hornblende
PFM002209A	6700651	1632580	B	Amphibolite	$^{40}Ar/^{39}Ar$ hornblende
PFM002210A	6700655	1632484	D	Granite dyke	U-Pb zircon
PFM002213A	6700532	1632663	C	Metagranodiorite	U-Pb zircon, $^{40}Ar/^{39}Ar$ biotite
PFM002216A	6699652	1630093	B	Metagabbro	U-Pb zircon, $^{40}Ar/^{39}Ar$ hornblende
PFM002217A	6698336	1634013	B	Metatonalite to metagranodiorite	U-Pb zircon
PFM002219A	6699506	1631340	B	Metagranite to metagranodiorite	$^{40}Ar/^{39}Ar$ biotite, (U-Th)/He apatite
PFM002219B	6699506	1631340	B	Amphibolite	$^{40}Ar/^{39}Ar$ hornblende
PFM002239A	6698839	1627369	B	Amphibolite	$^{40}Ar/^{39}Ar$ hornblende
PFM002241A	6697859	1634625	B	Amphibolite	$^{40}Ar/^{39}Ar$ hornblende
PFM002242A	6699917	1632853	B	Amphibolite	$^{40}Ar/^{39}Ar$ hornblende
PFM002244A	6698361	1633262	B	Amphibolite	$^{40}Ar/^{39}Ar$ hornblende
PFM002245A	6697733	1631685	B	Amphibolite	$^{40}Ar/^{39}Ar$ hornblende
KFM01A-100 (108.5-108.9 m)	6699529,8	1631397,2	B	Metagranite to metagranodiorite	$^{40}Ar/^{39}Ar$ biotite
KFM01A-200 (208.0-208.4 m)	6699529,8	1631397,2	B	Metagranite to metagranodiorite	(U-Th)/He apatite
KFM01A-400 (408.6-409.0 m)	6699529,8	1631397,2	B	Metagranite to metagranodiorite	(U-Th)/He apatite
KFM01A-600 (607.7-608.1 m)	6699529,8	1631397,2	B	Metagranite to metagranodiorite	(U-Th)/He apatite
KFM01A-800 (810.08-810.48 m)	6699529,8	1631397,2	B	Metagranite to metagranodiorite	(U-Th)/He apatite
KFM01A-1000 (1001.2-1001.6 m)	6699529,8	1631397,2	B	Metagranite to metagranodiorite	$^{40}Ar/^{39}Ar$ biotite, (U-Th)/He apatite

3 Equipment

3.1 Description of equipment/interpretation tools

The following equipment was used for sample collection in the field, sample crushing, mineral separation, and selection of individual minerals for analysis:

- Sledge hammer.
- Rock saw.
- Jaw-crusher.
- Swing-mill.
- Mill tray.
- Wilfley (water-shaking) table.
- Hand magnet.
- Frantz magnet separator.
- Heavy liquids (2-iodine methane).
- Plastic gloves.
- Binocular microscope.
- Tweezers.
- Jeol, JSM 6400 scanning microscope (University of Lund, Lund, Sweden).

The geochronological analyses were carried out using the instruments and laboratories listed below:

- Quadrupole mass spectrometer, Hal 51 (Free University, Amsterdam, Netherlands).
- HP4500 ICP-MS (Free University, Amsterdam, Netherlands).
- Cameca IMS 1270 ion microprobe (NORDSIM facility, Swedish Museum of Natural History, Stockholm, Sweden).
- Finnigan MAT262 mass spectrometer (University of Oslo, Oslo, Norway).
- Micromass 5400 mass spectrometer (University of Lund, Lund, Sweden).
- New Wave Research 50W CO_2 laser facility (University of Lund, Lund, Sweden).

4 Execution

4.1 Preparatory work

4.1.1. U-Pb (zircon, titanite) and $^{40}Ar/^{39}Ar$ hornblende dating

All rock samples were crushed by hand or with a jaw-crusher and subsequently milled using a swing-mill. Samples collected for U-Pb zircon and titanite analyses were processed into a fine powder because of the fine-grained nature of the target minerals. Heavy minerals, e.g. zircon and titanite, were separated from their lighter counterparts using a Wilfley water-shaking table. A hand magnet was used to remove magnetic phases and subsequently zircon and titanite were hand-picked under a binocular microscope.

Samples collected for $^{40}Ar/^{39}Ar$ hornblende analyses were processed into a range of grain-sizes to make sure that a selection of intact hornblende crystals remained. The resulting mix of grain-sizes was sieved under running water in order to divide each sample into fractions of >2 mm, 2–1 mm, 1–0.5 mm, 0.5–0.25 and <0.25 mm. The two fractions 1–0.5 mm and 0.5–0.25 mm were, in all cases, regarded as most likely to contain hornblende crystals suitable for analysis. The fractions were separated into one magnetic and one non-magnetic part using a Frantz magnetic separator. The non-magnetic parts of the two fractions were examined under a binocular microscope and hornblendes were hand-picked for analysis.

4.1.2 $^{40}Ar/^{39}Ar$ biotite and (U-Th)/He apatite dating

Samples selected for $^{40}Ar/^{39}Ar$ biotite analyses went through the same crushing procedure as the samples selected for apatite extraction and (U-Th)/He dating (see below). The lightest fraction (above clay fraction) was collected from the Wilfley table for biotite separation. The samples were sieved through a 500 µm mesh and biotites were hand-picked under a microscope from the largest fraction.

Apatite is an accessory mineral in most rock types. For this study, 0.5–1 kg of each rock sample was used. For mineral separation, each sample was reduced in size by a crushing procedure using a sledge hammer, a jaw-crusher and a mill tray. After these steps, each sample was placed on a Wilfley table to remove the clay size fraction. The two heaviest fractions from the Wilfley table were collected and dried. The samples were then sieved through a 250 µm and a 75 µm mesh and the middle fraction was placed into a heavy liquid (2-iodine methane, ∂=3.1 g/cm^3) to separate the apatite from lighter minerals such as feldspar and quartz. The heavy separate was placed through a Frantz magnet to remove all the magnetic minerals. All mineral separation was performed at the Department of Geosciences, University of Arizona, Tucson, Arizona, USA.

Euhedral to subhedral apatite grains were hand-picked. Investigation of the grains was performed under an high enlargement microscope to select those with no visible inclusions. Three to four single grains were then selected and a photographic record was compiled (see, for example, Figure 4-1).

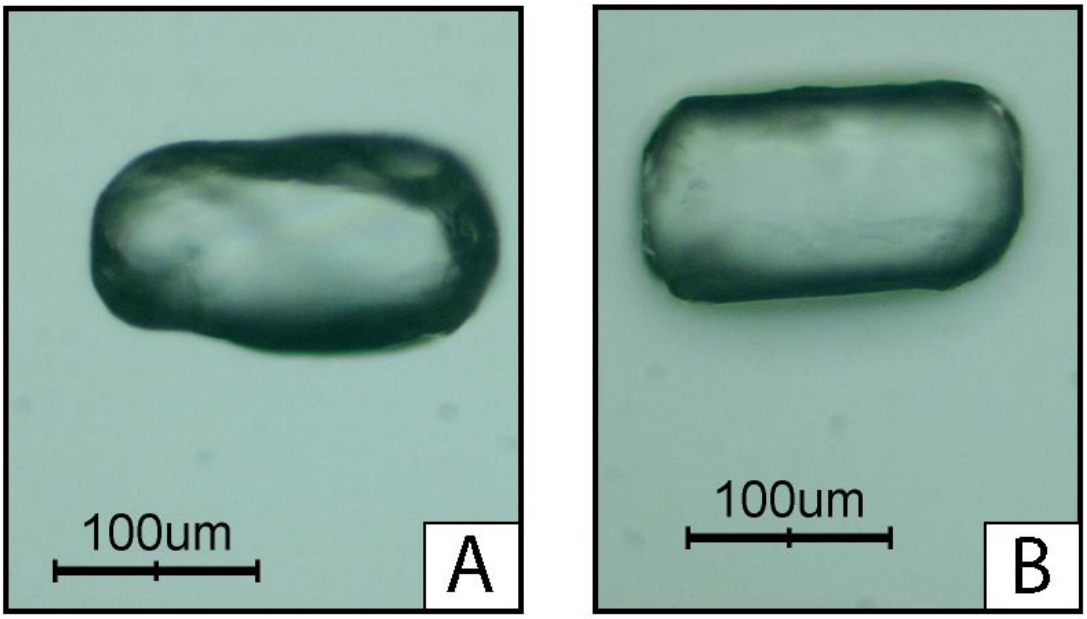

Figure 4-1. *Typical examples of selected apatites. Pictures shown are from the surface sample PFM002219A (left) and the sample from the c 400 m depth in KFM01A (right).*

4.2 Analytical work

4.2.1 U-Pb (zircon, titanite) geochronology

U-Pb geochronology has been carried out on four zircon samples (Figure 2-1) using the *S*econdary *I*on *M*ass *S*pectrometry (SIMS) technique at the Swedish Museum of Natural History in Stockholm, Sweden (NORDSIM facility). One zircon sample and two titanite samples (Figure 2-1) have also been analysed using the *T*hermal *I*onisation *M*ass *S*pectrometry (TIMS) technique at the University of Oslo, Norway. The TIMS work was carried out in close collaboration with Professor Fernando Corfu at the Department of Geosciences, University of Oslo, Norway.

SIMS technique

The hand-picked zircons were mounted in transparent epoxy resin together with chips of the 1065 Ma Geostandards zircon 91500 /Wiedenbeck et al, 1995/. The epoxy mount was polished sufficiently to expose any potentially older cores. Characterisation of the zircon structures was carried out using BSE- (Backscatter electron) and CL- (Cathodoluminescense) imaging. Prior to analysis, the mount was coated with c 30 nm of gold.

Ion-microprobe (SIMS) analyses were performed using the Cameca IMS 1270 high mass-resolution instrument at the NORDSIM facility. A c 4 nA O_2^- primary ion beam was used together with an aperture producing an ellipsoid analysis spot that is c 30 µm in size. The isotope masses were measured with an electron multiplier. Detailed analytical procedures are described by /Whitehouse et al, 1997, 1999/.

TIMS technique

The grains of zircon and titanite from each selected sample were grouped into three or more fractions based on degree of alteration, abundance of micro-cracks, crystal shape and crystal colour. All fractions, except one (067/S.08), were then abraded to remove external disturbed domains /Krogh, 1982; Davis et al, 1982/. The selected samples were subsequently washed using HNO_3, H_2O and acetone, weighed on a microbalance and spiked with a mixed $^{205}Pb/^{235}U$ tracer. Zircons were dissolved with HF (+HNO_3) in Teflon bombs /Krogh, 1973/ at 185–190°C, whereas dissolution of titanite was carried out in Savillex vials on a hot plate. Chemical purification was performed on all samples except zircons with a weight of less than 5 µg. Mini-columns, with an anion exchange resin (Dowex AG 1X-8, 200–400 mesh), were used on all processed fractions except one (057/S.57), where a large column was used. The zircons were processed with HCl /modified from Krogh, 1973/ and the titanites using a single stage technique with 3 N HCl + 0.5 N HBr /Corfu and Andersen, 2002/. The residual HBr in the titanite columns was removed from the resin by passing through 3 N HCl. The Pb and U were then collected with 6 N HCl and H_2O, respectively. The purified Pb and U were loaded together on outgassed Re filaments with Si-gel and phosphoric acid.

Analyses were carried out with a Finnigan MAT262 mass spectrometer either in static mode on Faraday cups, or for small amounts and all $^{207}Pb/^{204}Pb$ ratios, in dynamic mode using an electron multiplier (EM). The data were corrected for 0.1%/amu fractionation on both Pb and U, with an additional bias correction for EM data determined from regular runs of the NBS 982 Pb standard. Blank correction was 2 pg Pb and 0.1 pg U, and the initial Pb was corrected using Pb compositions calculated with the /Stacey and Kramers, 1975/ model. More detailed descriptions of the analytical procedures are given by /Corfu and Andersen, 2002/ and /Corfu, in press/.

4.2.2 $^{40}Ar/^{39}Ar$ (hornblende, biotite) geochronology

$^{40}Ar/^{39}Ar$ geochronology has been carried out on nine hornblende samples and eight biotite samples (Figure 2-1) at the new $^{40}Ar/^{39}Ar$ geochronological laboratory at the University of Lund, Sweden.

The hornblende and biotite samples selected for $^{40}Ar/^{39}Ar$ geochronology were irradiated together with the DRA-1 sanidine standard (25.26 Ma) /Wijbrans et al, 1995/, recalculated following /Renne et al,1998/, for 35 hours at the NRG-Petten HFR RODEO facility in the Netherlands. J-Values were calculated with a precision of 0.5%.

The $^{40}Ar/^{39}Ar$ geochronology laboratory at the University of Lund contains a Micromass 5400 mass spectrometer with a Faraday and an electron multiplier. A metal extraction line, which contains two SAES C50-ST101 Zr-Al getters and a cold finger cooled to ca –155°C by a Polycold P100 cryogenic refrigeration unit, is also present. One or two grains of hornblende or biotite were loaded into a copper planchette that consists of several 3 mm holes. Samples were step-heated using a defocused 50W CO_2 laser. Sample clean-up time that made use of the two hot Zr-Al SAES getters and a cold finger with a Polycold refrigeration unit was five minutes. The laser was rastered over the samples to provide even-heating of all grains. The entire analytical process is automated and runs on a Macintosh-steered OS 10.2 with software modified specifically for the laboratory at the University of Lund and developed originally at the Berkeley Geochronology Center (Al Deino).

Time zero regressions were fitted to data collected from 10 scans over the mass range of 40 to 36. Peak heights and backgrounds were corrected for mass discrimination, isotopic decay and interfering nucleogenic Ca-, K-, and Cl-derived isotopes. Isotopic production values for the cadmium-lined position in the Petten reactor are $^{36}Ar/^{37}Ar(Ca) = 0.000270$, $^{39}Ar/^{37}Ar(Ca) = 0.000699$, and $^{40}Ar/^{39}Ar(K) = 0.00183$. ^{40}Ar blanks were calculated before every new sample and after every three sample steps.^{40}Ar blanks were between $6.0–3x10^{-16}$. Blank values for masses 39–36 were all less than $7x10^{-18}$. Blank values were subtracted for all incremental steps from the sample signal. The laboratory was able to produce very good incremental gas splits, using a combination of increasing time at the same laser output, followed by increasing laser output. Age plateaus were determined using the criteria of /Dalrymple and Lamphere, 1971/, which specify the presence of at least three contiguous incremental heating steps with statistically indistinguishable ages and constituting greater than 50% of the total ^{39}Ar released during the experiment. Inverse isochrons yield ages statistically indistinguishable from those given by the plateaus and are not presented here.

4.2.3 (U-Th)/He thermochronology

(U-Th)/He thermochronology has been carried out on seven apatite samples at the Forsmark site (Figure 2-1). Final hand-picking of the apatites selected for analysis and all the analyses were performed in close collaboration with Dr. Joaquim Juez-Larré at the Free University, Amsterdam, Netherlands.

Helium extraction

Helium measurements were conducted on a quadruple mass spectrometer. For each individual sample, the single apatite grain was inserted in an inconel capsule and loaded into separate inconel tubes attached to a thermocouple. The inconel tubes were mounted in a flange multiplexer and pumped to UHV-conditions. First, a hot blank was measured to ensure the absence of helium or a leak in the system. Next the first inconel tube containing a sample was heated in an external oven for 30 minutes up to 900°C. These T-t conditions guarantee the complete extraction of helium from the apatite grain size used in this study. After degassing and before the helium was measured, a sequential clean-up procedure was carried out, consisting of:

1. Exposure to a SAES getter at 450°C for the removal of reactive gases.
2. Exposure to one charcoal trap held at nitrogen temperatures to remove non-reactive condensable gases.
3. Exposure to a SAES getter at 20°C for absorption of H_2.

The remaining helium fraction was then expanded into the mass spectrometer for analysis. The amount of helium was determined by counts per second compared to an internal standard (Krusivik geothermal gas) measured under the same conditions as the analysed sample. One shot of Krusivik typically contains $(2.60±0.02)x10^{-7}$ cm^3 of ^{4}He at STP.

U-Th measurements

The grains were unloaded from the inconel capsules and the apatite was transferred to a Teflon beaker. Grains were dissolved with HNO_3 and HF on hot plates, spiked with two artificial isotopes (^{233}U and ^{229}Th) and diluted up to ~3 ml with MiliQwater. In this solution, the uranium and thorium contents were measured using an **I**nductively **C**oupled **P**lasma **M**ass **S**pectrometer (ICP-MS). The argon ICP used is a high temperature plasma fireball,

into which the aerosol sample is carried by argon gas. A low-flow Teflon nebulizer (90–120 µl/min) was used in order to increase the ICP-MS efficiency for measurements of very low U-Th concentrations in small quantities of the solution. The plasma decomposes and dissociates the particles of the sample and then ionises the resulting atoms. The ions were partially extracted into the vacuum chamber, focused and transferred to a quadruple mass spectrometer, where they were analysed by an electron multiplier detector in a rapid sequential scan. Detection limits are typically at the ng/l (ppt) level. The resulting mass spectra were used to quantify the amount of ^{238}U and ^{232}Th by isotopic ratio comparison to the two artificial isotopes of known concentration.

Durango standard calibration

Verification of the analytical technique and procedures is provided by routine analyses of an apatite standard. As a standard we used the 160–180 µm fraction of crushed and sieved Durango apatite crystals that were originally 1–2 cm in size. Each standard aliquot comprised from 1 to 50 grains. Six standards were measured for (U-Th)/He in the analyses, containing between 0.147 and 0.006 mgr of Durango apatite grains. The results yielded a range of (U-Th)/He ages between 28±1 Ma and 35±1 Ma against a reported age of 32±1 Ma /Farley, 2000; Jonckheere et al, 1993/.

4.3 Data Handling

The program Isoplot/Ex 3.00 /Ludwig, 2003/ has been used for calculating ages and plotting the data obtained from the SIMS and TIMS analyses. $^{40}Ar/^{39}Ar$ geochronology data were produced, plotted and fitted using the argon programme provided by Al Deino from the Berkeley Geochronology Centre, USA. Data was subsequently exported to MS Excel tables. (U-Th)/He ages were calculated with an in-house program used at the Free University, Amsterdam, Netherlands. Data was subsequently exported to MS Excel tables.

5 Results

The data from the geochronological study are presented in tables, one for each technique. These data contain the information that is needed to calculate the various ages. The data are also presented in plots that are appropriate for the different techniques. Tera-Wasserburg and conventional concordia diagrams are used for the U-Pb (SIMS) and U-Pb (TIMS) data, respectively, and step-heating spectra for all the $^{40}Ar/^{39}Ar$ data. The (U-Th)/He data are plotted in an age–depth diagram.

5.1 U-Pb (zircon, titanite) ages

In the case of the U-Pb isotope system, an age can be calculated as a concordia age, a concordia intercept, or as a weighted average of $^{207}Pb/^{206}Pb$ ages. A concordia age can be calculated when the data are concordant, i.e. lie on the concordia curve, and it integrates the $^{206}Pb/^{238}U$, $^{207}Pb/^{235}U$ and $^{207}Pb/^{206}Pb$ ages. A drawback is that a small deviation from concordance can affect the age depending on the slope of the concordia curve. A concordia intercept is the intersection between the concordia and a discordia line. This line is defined by a set of discordant data, which is the result of lead loss in the analysed crystals. In this study, we have preferred to use the weighted average of the $^{207}Pb/^{206}Pb$ ages for concordant data, since it is not sensitive to deviations from concordance produced by recent lead loss. It should be noted that some of the ages presented in the concordia diagrams are in fact weighted averages.

Following data acquisition with the help of the SIMS technique, it was evident that the analytical points within two of the samples, PFM002207A and PFM002213A, showed a statistically significant spread, with a few analyses considerably older than the majority of the analyses. To deal with this problem, the internal structures of the zircons were studied in the BSE- and CL-images. Zircons with magmatic oscillatory zoning were selected in favour of altered zircons that lack zoning or show BSE-bright, or CL-dark images (Figures 5-1 and 5-2, respectively). This approach works well since some of the worst outliers are discarded. However, it also means that a few analyses that are consistent with the majority of analyses have been omitted from the age calculations.

5.1.1 U-Pb (zircon) ages based on the SIMS technique

The data that have been derived with the help of the U-Pb SIMS technique and that have been used to calculate the four ages presented here are listed in Table 5-1. All samples are from the surface. A short summary of the results for each sample is presented below.

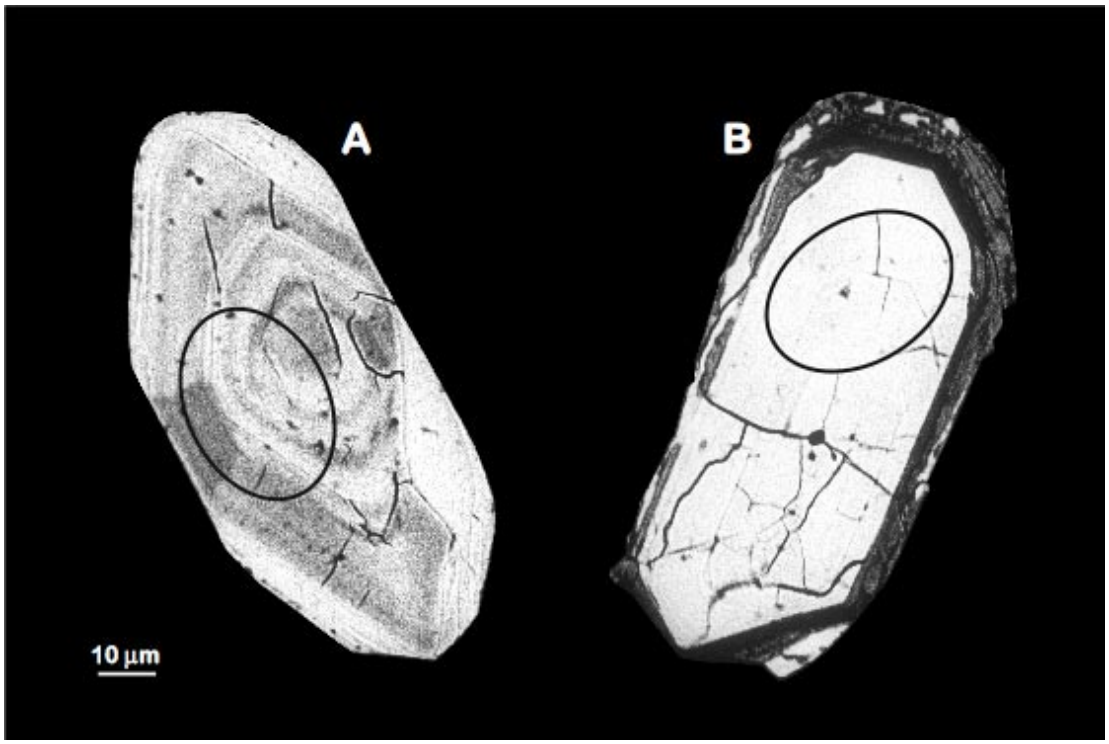

Figure 5-1. *Representative BSE-images of zircons mounted for analysis by the SIMS technique. A: Zircon (analysis n1257-07a) with magmatic oscillatory zoning that has been included in an age calculation. B: Zircon (analysis n1257-06a) that lacks zoning, is BSE-bright and has been omitted from an age calculation. Ellipses mark analysed spots.*

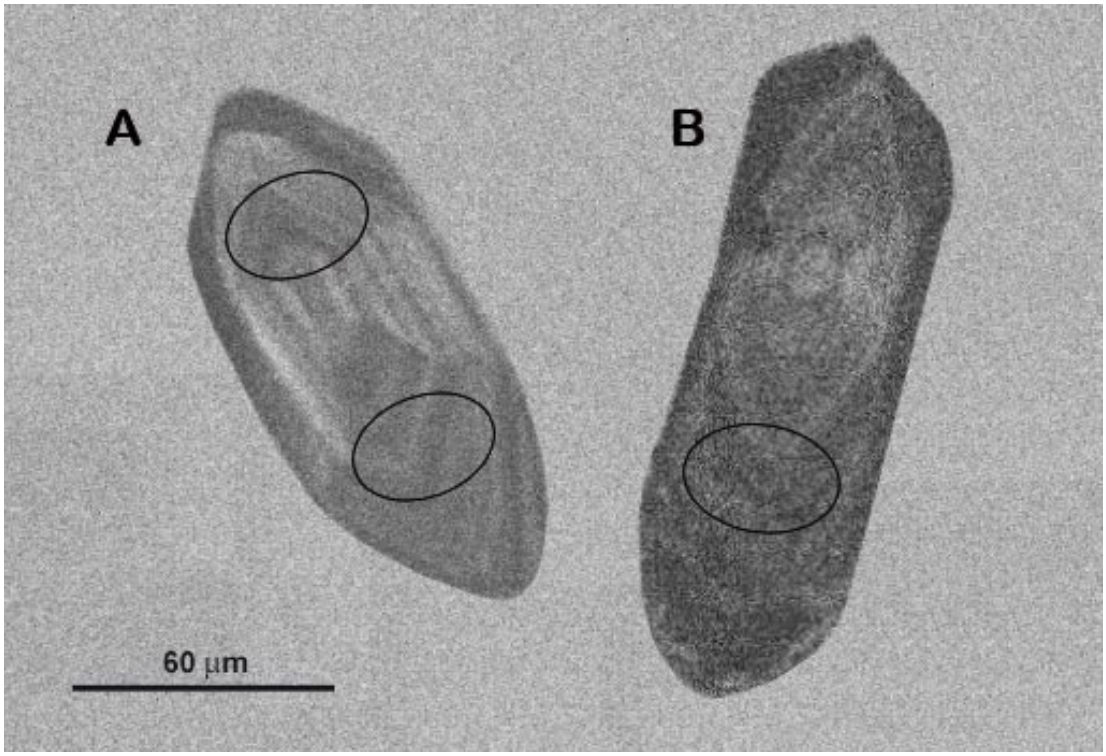

Figure 5-2. *Representative CL-images of zircons mounted for analysis by the SIMS technique. A: Zircon (analyses n1425-12b and n1425-12a) with magmatic oscillatory zoning that has been included in an age calculation. B: Zircon (analysis n1425-03a) with altered zoning and CL-dark image that has been omitted from an age calculation. Ellipses mark analysed spots.*

Table 5-1. U-Pb (zircon) data derived with the help of the SIMS technique.

Sample/ spot	Structural class[c] (from CL and BSE)	Pb (ppm)	U (ppm)	Th/U measured	$^{206}Pb/^{204}Pb$ measured	f^{d}_{206} %	$^{206}Pb/^{238}U$	±σ %	$^{207}Pb/^{206}Pb$	±σ %	$^{206}Pb/^{238}U$ age (Ma)	±σ	$^{207}Pb/^{206}Pb$ age (Ma)	±σ	Conc.[e] %
PFM002207A. Weighted average of 207Pb/206Pb ages: 1865 ± 3,4, MSWD 0,83															
n1257-01a	BSE sl al zon	201	476	0,33	53509	0,03	0,3492	1,9	0,1146	0,31	1931	31	1874	5,5	103
n1257-01b	BSE sl al zon	137	334	0,50	19846	0,09	0,3225	1,9	0,1137	0,36	1802	29	1860	6,5	96
n1257-02a	BSE osc zon	168	421	0,33	39098	0,05	0,3286	1,9	0,1141	0,30	1832	30	1866	5,5	98
n1257-03a	BSE osc zon	189	455	0,46	27718	0,07	0,3332	1,9	0,1137	0,44	1854	30	1859	7,9	100
n1257-03b	BSE osc zon	218	525	0,37	12274	0,15	0,3388	1,9	0,1141	0,33	1881	30	1866	5,9	101
n1257-04a[a]	BSE hom	190	445	0,31	67692	0,03	0,3546	1,9	0,1153	0,38	1956	31	1884	6,9	104
n1257-05a[a]	BSE-bright wk zon	200	491	0,37	39953	0,05	0,3335	1,9	0,1156	0,35	1855	30	1889	6,2	98
n1257-06a[a]	BSE-bright hom	236	561	0,34	34744	0,05	0,3466	1,9	0,1169	0,56	1918	31	1909	10	101
n1257-07a	BSE osc zon	144	342	0,47	18197	0,1	0,3395	1,9	0,1135	0,42	1884	30	1856	7,6	102
n1257-08a[b]	BSE sl al zon	108	286	0,59	3851	0,49	0,3027	5,7	0,1122	1,2	1705	86	1835	22	92
n1257-09a[b]	BSE sl al zon	196	455	0,83	7930	0,24	0,3278	5,7	0,1131	1,2	1828	91	1850	21	99
n1257-10a[ab]	BSE wk zon al	139	388	0,49	2677	0,7	0,2959	5,7	0,1104	1,4	1671	85	1806	25	92
n1427-01a	CL osc zon	118	286	0,36	54707		0,3386	1,7	0,1143	0,44	1880	28	1869	7,9	101
n1427-02a	CL osc zon	92	227	0,33	28400	0,07	0,3367	1,7	0,1136	0,47	1871	28	1859	8,5	101
n1427-03a	CL osc zon	141	349	0,34	38340	0,05	0,3328	1,7	0,1140	0,38	1852	27	1865	6,8	99
n1427-04a	CL osc zon	98	244	0,33	52238		0,3319	1,7	0,1146	0,44	1847	27	1874	7,8	98
n1427-05a	CL osc zon	153	376	0,40	52948	0,04	0,3313	1,7	0,1136	0,36	1844	27	1858	6,4	99
n1427-06a	CL osc zon	115	310	0,35	56022		0,3046	1,7	0,1147	0,44	1714	26	1875	7,9	90
n1427-07a	CL osc zon	112	286	0,45	12575	0,15	0,3159	1,7	0,1141	0,43	1769	26	1866	7,8	94
n1427-08a	CL osc zon	167	408	0,55	24416	0,08	0,3227	1,7	0,1139	0,37	1803	27	1863	6,7	96
n1427-09a[a]	CL-dark hom	220	574	0,06	102659		0,3381	1,7	0,1148	0,29	1878	28	1876	5,2	100
n1427-09b	CL osc zon	152	391	0,33	53995	0,03	0,3222	1,7	0,1137	0,38	1801	27	1860	6,9	96

PFM002210A. Weighted average of 207Pb/206Pb ages: 1851± 5,2, MSWD 0,22

n1259-01a	BSE hom	100	234	0,38	23363	0,08	0,3485	1,9	0,1130	0,47	1927	31	1849	8,5	105
n1259-02a	BSE wk osc zon	62	149	0,35	9444	0,2	0,3420	1,9	0,1130	0,63	1896	31	1848	11	103
n1259-03a	BSE zon	265	605	0,33	44276	0,04	0,3633	1,9	0,1134	0,44	1998	32	1854	7,9	109
n1259-04a	BSE-bright hom	531	1254	0,37	18906	0,1	0,3479	1,9	0,1132	0,47	1925	31	1851	8,4	105
n1259-04b	BSE-bright wk zon	418	977	0,36	24542	0,08	0,3516	1,9	0,1133	0,37	1942	31	1852	6,6	106
n1259-05a	BSE wk zon	274	662	0,24	35132	0,05	0,3502	1,9	0,1133	0,49	1935	31	1853	8,9	105
n1259-07a	BSE hom	400	928	0,30	37152	0,05	0,3621	1,9	0,1128	0,53	1992	32	1844	9,5	109
n1259-08a	BSE hom	140	326	0,27	21118	0,09	0,3630	1,9	0,1132	0,64	1997	32	1851	12	109
n1259-09a	BSE hom	453	998	0,50	54964	0,03	0,3625	1,9	0,1132	0,41	1994	32	1852	7,3	109
n1259-10a	BSE hom	508	1225	0,30	47965	0,04	0,3470	1,9	0,1133	0,53	1920	31	1854	9,5	104
n1429-01a	BSE-dark hom	68	165	0,37	21554	0,09	0,3386	1,7	0,1124	0,59	1880	28	1839	11	103

PFM002213A. Weighted average of 207Pb/206Pb ages: 1864 ± 3,4, MSWD 1,4

n1258-01a	BSE osc zon	147	327	0,47	45756	0,04	0,3595	1,9	0,1142	0,42	1980	32	1867	7,5	107
n1258-02a[a]	BSE-bright hom	324	737	0,48	50418	0,04	0,3530	1,9	0,1165	0,33	1949	32	1904	5,9	103
n1258-02b[a]	BSE-bright hom	200	502	0,30	9245	0,2	0,3329	1,9	0,1155	0,37	1852	31	1887	6,6	98
n1258-03a[a]	BSE-bright hom	219	523	0,33	17984	0,1	0,3467	1,9	0,1157	0,32	1919	31	1890	5,8	102
n1258-04a[a]	BSE-bright hom	174	412	0,31	45286	0,04	0,3523	1,9	0,1160	0,35	1946	31	1896	6,3	103
n1258-05a	BSE wk osc zon	140	340	0,30	8864	0,21	0,3453	1,9	0,1140	0,56	1912	31	1864	10	103
n1258-06a	BSE wk osc zon	148	359	0,30	17325	0,11	0,3446	1,9	0,1146	0,54	1909	31	1874	9,7	102
n1258-07a	BSE osc zon	175	445	0,40	10586	0,18	0,3198	1,9	0,1134	0,44	1789	29	1855	7,9	96
n1258-08a[a]	BSE-bright wk zon	261	605	0,38	20455	0,09	0,3531	1,9	0,1157	0,40	1949	31	1891	7,3	104
n1425-01a	CL osc zon	168	390	0,62	104203		0,3341	1,2	0,1141	0,36	1858	20	1865	6,6	100
n1425-03a[a]	CL-dark al zon	349	1074	0,57	7272	0,26	0,2581	1,5	0,1091	0,30	1480	20	1784	5,5	81
n1425-04a	CL osc zon	126	313	0,51	20834	0,09	0,3198	1,5	0,1143	0,52	1789	23	1869	9,3	95
n1425-05a	CL osc zon	145	353	0,42	13282	0,14	0,3337	1,5	0,1139	0,39	1856	24	1863	7,1	100
n1425-06a	CL osc zon	128	306	0,50	37541	0,05	0,3338	1,5	0,1141	0,39	1857	24	1865	7,1	100
n1425-07a	CL osc zon	172	400	0,67	9424	0,2	0,3296	1,5	0,1143	0,38	1836	24	1869	6,8	98
n1425-08a	CL osc zon	152	373	0,42	145941		0,3314	1,5	0,1144	0,35	1845	24	1870	6,4	98
n1425-09a	CL osc zon	182	455	0,46	31901	0,06	0,3203	1,5	0,1132	0,43	1791	23	1852	7,7	96
n1425-10a	CL osc zon	258	640	0,38	15273	0,12	0,3312	1,5	0,1138	0,29	1844	24	1862	5,2	99
n1425-11a	CL osc zon	197	465	0,61	46271	0,04	0,3292	1,5	0,1145	0,32	1834	24	1872	5,7	98

n1425-12a	CL osc zon	132	327	0,37	53307		0,3315	1,5	0,1143	0,37	1846	24	1869	6,7	99
n1425-12b	CL osc zon	109	276	0,34	19590	0,1	0,3275	1,5	0,1135	0,48	1826	24	1857	8,6	98
n1425-13a	CL osc zon	210	497	0,57	32073	0,06	0,3300	1,5	0,1143	0,31	1839	24	1868	5,6	98
n1425-14a	CL osc zon	305	830	0,43	19901	0,09	0,2978	1,5	0,1132	0,25	1681	22	1852	4,6	90
n1428-01a	CL sl al wk zon	177	516	0,41	3186	0,59	0,2725	1,7	0,1135	0,53	1553	24	1856	9,5	82
n1428-01b	CL osc sect zon	95	283	0,35	488	3,83	0,2671	1,8	0,1130	1,2	1526	25	1848	21	80
n1428-01c	CL wk zon	449	1021	0,74	18599	0,1	0,3277	1,7	0,1143	0,25	1827	27	1869	4,4	97
n1428-02a	CL wk zon	136	346	0,31	22053	0,08	0,3258	1,7	0,1124	0,48	1818	27	1839	8,7	99
n1428-02b	CL wk zon	130	323	0,30	88558		0,3331	1,7	0,1135	0,46	1853	27	1857	8,2	100
n1428-03a	CL sl al zon	173	410	0,51	38616	0,05	0,3319	1,7	0,1149	0,38	1848	27	1878	6,9	98
n1428-04a	CL osc zon	95	223	0,47	32083	0,06	0,3388	1,7	0,1142	0,56	1881	28	1868	10	101
n1428-04b	CL osc zon	176	405	0,59	151306		0,3388	1,7	0,1141	0,35	1881	28	1866	6,3	101
PFM002217A. Weighted average of 207Pb/206Pb ages: 1883 ± 3,1, MSWD 0,97															
n1426-01a	CL wk osc zon	164	398	0,27	101870		0,3448	1,7	0,1156	0,35	1910	28	1890	6,2	101
n1426-01b	CL wk osc zon	164	407	0,24	15684	0,12	0,3408	1,7	0,1150	0,42	1890	28	1879	7,6	101
n1426-02a	CL wk osc zon	182	441	0,31	74561		0,3422	1,7	0,1160	0,36	1897	28	1895	6,5	100
n1426-02b	CL wk osc zon	182	442	0,31	52526	0,04	0,3429	1,7	0,1146	0,37	1901	28	1874	6,6	102
n1426-03a	CL wk osc zon	255	598	0,41	178815		0,3463	1,7	0,1150	0,30	1917	28	1881	5,3	102
n1426-04a	CL wk osc zon	206	502	0,34	25655	0,07	0,3392	1,7	0,1148	0,39	1883	28	1877	7,1	100
n1426-05a	CL wk osc zon	344	806	0,41	578422		0,3465	1,7	0,1152	0,24	1918	28	1883	4,4	102
n1426-05b	CL wk osc zon	312	734	0,41	161592		0,3451	1,7	0,1150	0,25	1911	28	1880	4,5	102
n1426-06a	CL wk osc zon	217	514	0,35	85339		0,3466	1,7	0,1149	0,33	1919	28	1878	5,9	102
n1426-07a	CL wk osc zon	201	483	0,37	62622	0,03	0,3410	1,7	0,1154	0,31	1892	28	1886	5,6	100
n1426-07b	CL wk osc zon	189	454	0,37	60881	0,03	0,3414	1,7	0,1151	0,33	1893	28	1882	5,9	101
n1426-08a	CL wk osc zon	178	427	0,32	68347		0,3455	1,7	0,1158	0,38	1913	28	1892	6,8	101
n1426-08b	CL wk osc zon	214	531	0,36	33490	0,06	0,3319	1,7	0,1149	0,31	1848	27	1878	5,7	98

[a] Omitted from age calculation

[b] Small spot size (c 10 µm)

[c] CL, Cathodoluminescens imaging; BSE, Back scatter electron imaging; zon, zoning; osc, oscillatory; sect, sectorial; hom, homogeneous; wk, weak; al, altered; sl, slightly

[d] Percentage of ^{206}Pb contributed by common Pb, estimated from ^{204}Pb and assuming Stacey and Kramers (1975) model. Blanks indicate no detectable contribution

[e] Degree of concordance; numbers >100% are reversed discordant

PFM002207A

Sample PFM002207A is a Group B, medium-grained metagranite from an outcrop inside the candidate area (Figure 1-2). The metagranite shows a linear grain-shape fabric and a weaker planar grain-shape fabric. All these structures formed under amphibolite-facies metamorphic conditions.

The age obtained, 1865±3.4 Ma, is a weighted average of the $^{207}Pb/^{206}Pb$ ages and is interpreted as the age of crystallisation of the granite pluton (Figure 5-3). It is evident that some of the analysed crystals are slightly discordant due to recent lead loss (Figure 5-3). Since there are insufficient discordant data to construct a reliable discordia line, no attempt has been made to calculate an intercept age.

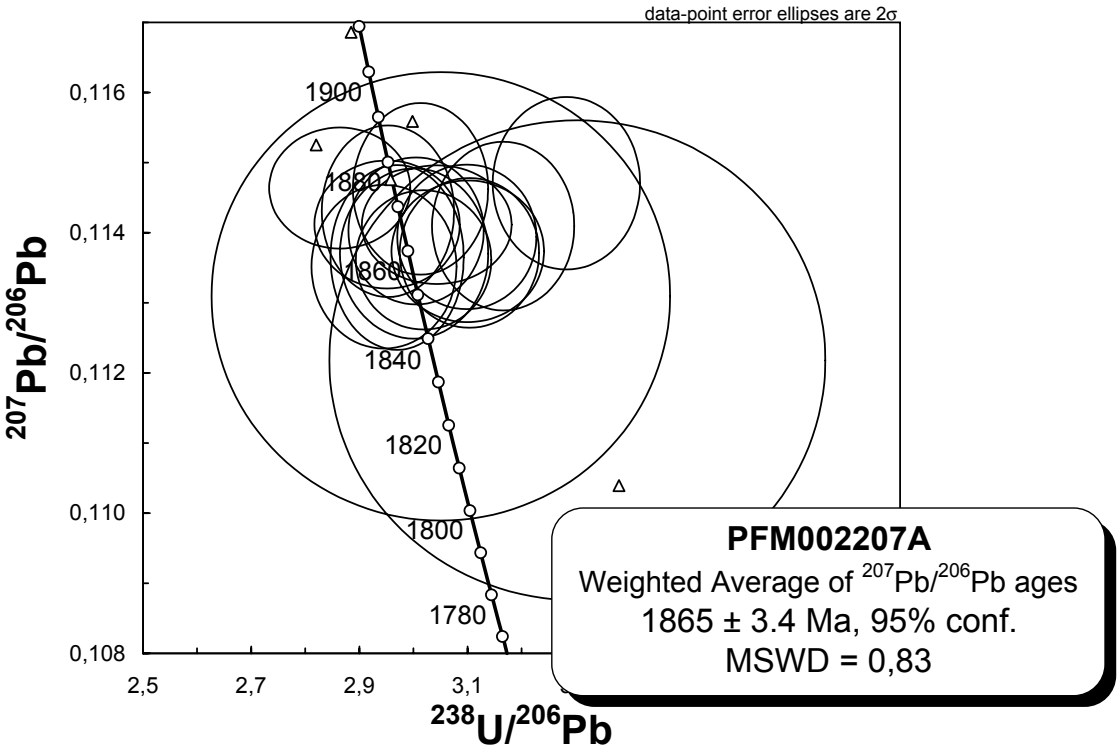

Figure 5-3. *Tera-Wasserburg concordia diagram for sample PFM002207A. Triangles indicate the positions of analyses omitted from the age calculation.*

PFM002210A

Sample PFM002210A is a Group D granite dyke from a coastal outcrop on Klubbudden that is situated northeast of the candidate area (Figure 1-2). The dyke is strongly discordant to a tectonic banding in the surrounding host rocks that is defined primarily by different components of Group B meta-intrusive rocks. On a larger scale, the tectonically banded sequence is folded and the outcrop from which this sample has been taken is situated on the northeastern limb of a major synform that plunges moderately to the south-east.

The age obtained, 1851±5.2 Ma, is a weighted average of the $^{207}Pb/^{206}Pb$ ages and is interpreted as the age of crystallisation. The fact that the analyses are slightly reversed discordant is an analytical artefact and does not affect the $^{207}Pb/^{206}Pb$ ages.

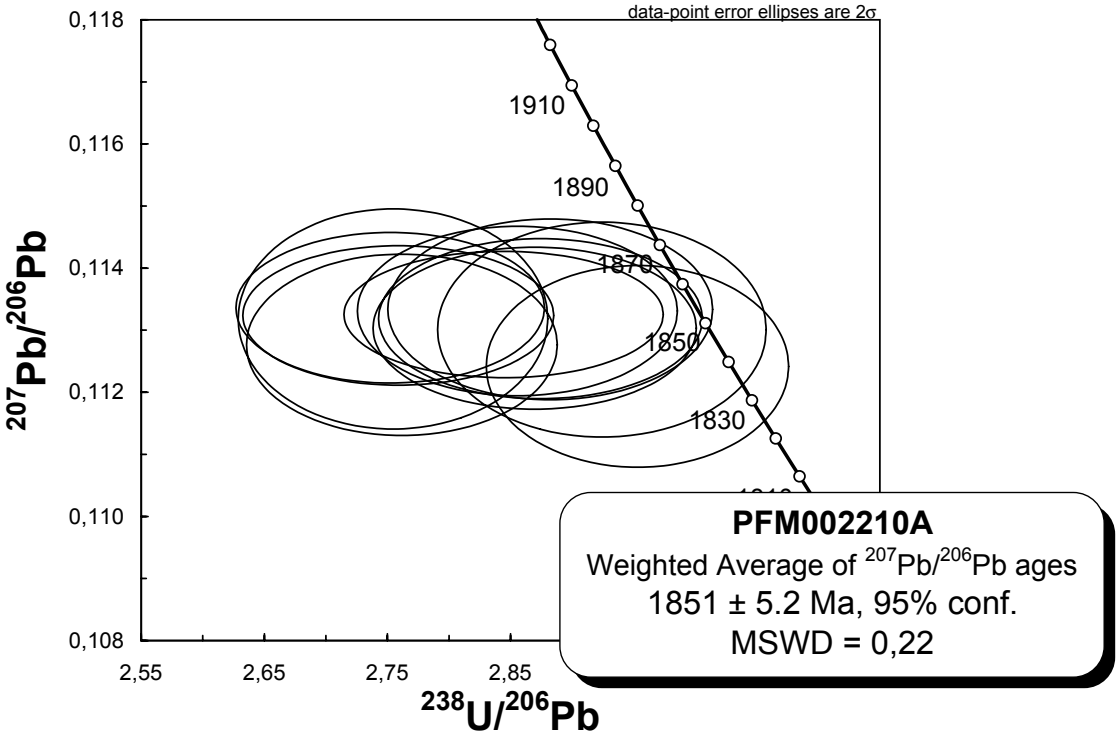

Figure 5-4. *Tera-Wasserburg concordia diagram for sample PFM002210A.*

PFM002213A

Sample PFM002213A is a Group C metagranodiorite from a coastal outcrop on Klubbudden that is situated northeast of the candidate area (Figure 1-2). The metagranodiorite is slightly discordant to the same tectonic banding described above. The metagranodiorite shows a linear grain-shape fabric that developed under lower amphibolite-facies metamorphic conditions.

The age obtained, 1864±3.4 Ma, is a weighted average of the $^{207}Pb/^{206}Pb$ ages and is interpreted as the age of crystallisation of the metagranodiorite (Figure 5-5). It is evident that some of the analysed crystals are slightly discordant, due to recent lead loss (Figure 5-5). However, there are not enough discordant data to construct a reliable discordia line. For this reason, no attempt has been made to calculate an intercept age.

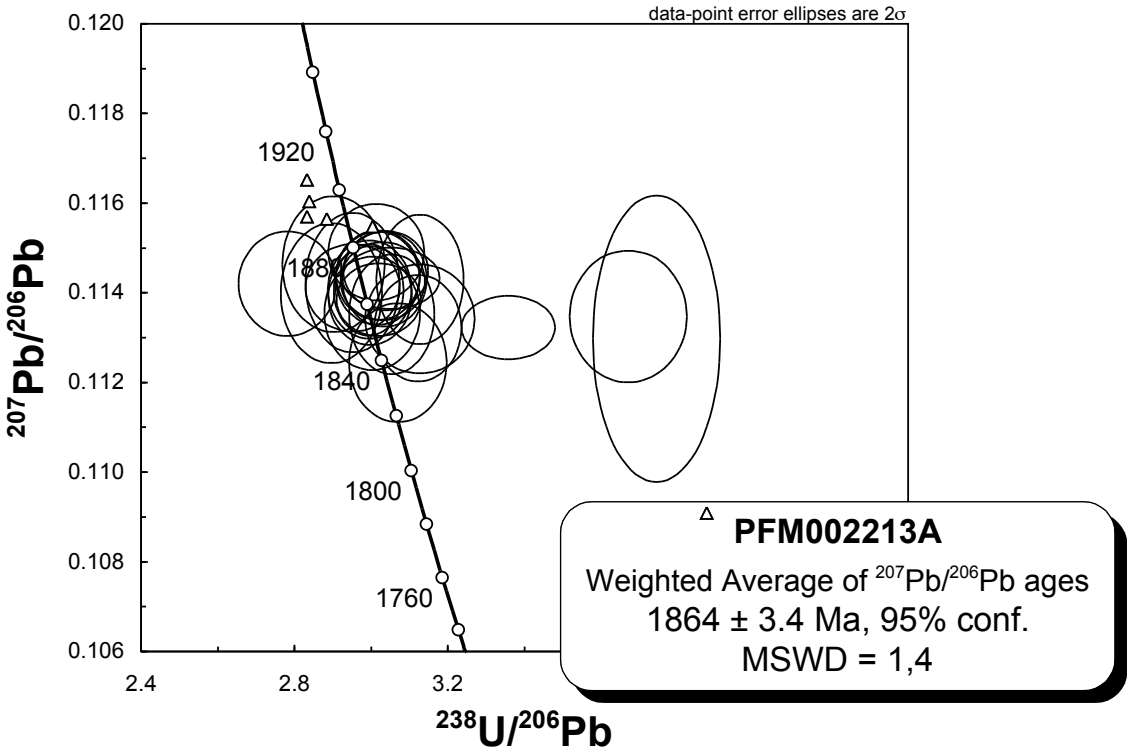

Figure 5-5. *Tera-Wasserburg concordia diagram for sample PFM002213A. Triangles indicate the positions of analyses omitted from the age calculation.*

PFM002217A

Sample PFM002217A is from a Group B metatonalite to metagranodiorite pluton that is situated partially inside the candidate area (Figure 1-2). On the basis of a modal analysis /Stephens et al, 2003b/, this sample is inferred to be granodioritic in composition. The metatonalite to metagranodiorite pluton shows a strong linear and a somewhat weaker planar grain-shape fabric. This mineral fabric developed under amphibolite-facies metamorphic conditions.

The age obtained, 1883±3.1 Ma, is a weighted average of the $^{207}Pb/^{206}Pb$ ages and is interpreted as the age of crystallisation of the Group B metatonalite to metagranodiorite body (Figure 5-6). Calculation of a concordia age provides the same result.

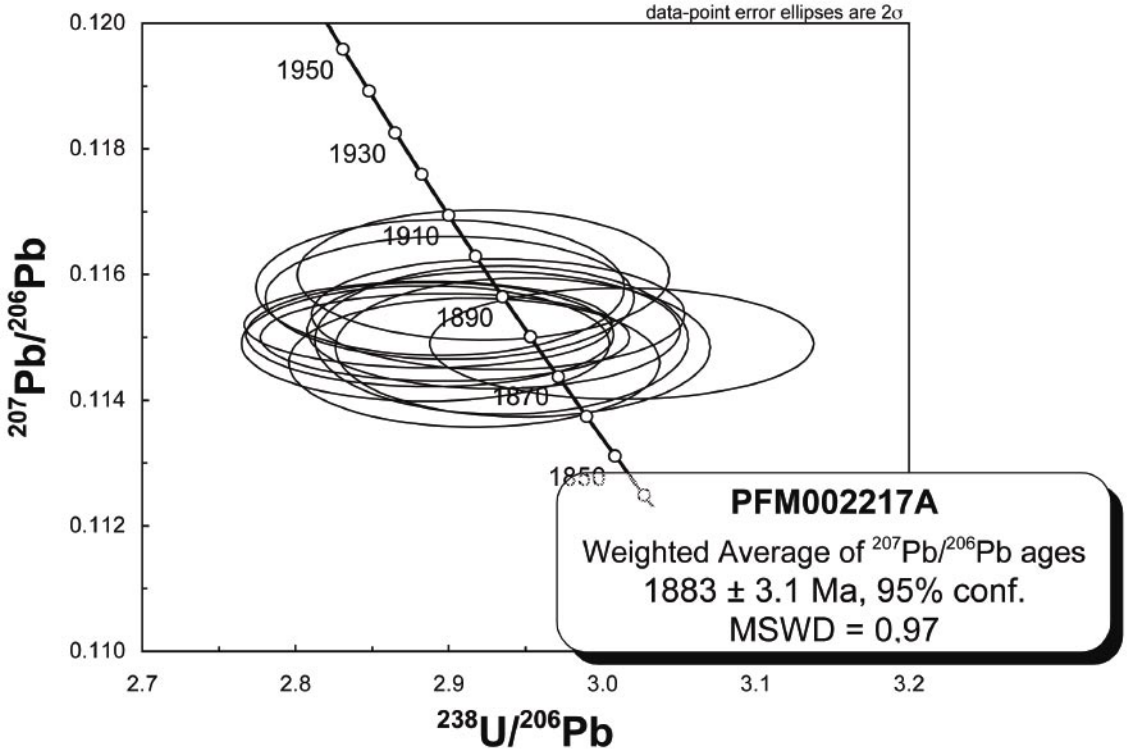

Figure 5-6. *Tera-Wasserburg concordia diagram for sample PFM002217A.*

5.1.2 U-Pb (zircon, titanite) ages based on the TIMS technique

The data that have been derived with the help of the U-Pb TIMS technique and that have been used to calculate the three ages presented here are listed in Table 5-2. All samples are from the surface. A short summary of the results for each sample is presented below.

Table 5-2. U-Pb (zircon, titanite) data derived with the help of the TIMS technique.

Sample/fraction analysed	Mineral-characteristics[b]	Weight[c] (ug)	Pb[c] (ppm)	U[c] (ppm)	Th/U[d]	Pbc[e] (ppm)	(pg)	$^{206}Pb/^{204}Pb$[f]	$^{207}Pb/^{235}U$[g]	2 σ	$^{206}Pb/^{238}U$[g]	2 σ	ρ	$^{206}Pb/^{238}U$[g] age (Ma)	$^{207}Pb/^{235}U$[g] age (Ma)	$^{207}Pb/^{206}Pb$[g] age (Ma)	2 σ[h]	Conc.[i] (%)
PFM000718G. Concordia upper intercept at 1844 ± 4 Ma, MSWD = 0,0018																		
057/S.57	T fr b-pb tl (n=25)	160	51	136	0,62	1,42	248,5	1806	5,034	0,016	0,32566	0,00093	0,93	1817,3	1825,0	1833,9	2,1	99
057/S.53	T fr b tl (n=2)	25	50	133	0,65	1,06	30,8	2215	5,006	0,014	0,32429	0,00083	0,93	1810,6	1820,3	1831,4	2,0	99
067/S.04	T fr b(-rb) tl (n=6)	12	64	170	0,60	1,13	16,8	2539	5,163	0,017	0,33190	0,00100	0,90	1847,6	1846,5	1845,2	2,5	100
067/S.06	T fr b(-rb) tl (n=11)	26	58	157	0,59	0,93	28,2	2977	5,055	0,013	0,32669	0,00074	0,94	1822,3	1828,6	1835,8	1,6	99
067/S.03[a]	T fr b(-rb) al (n=9)	125	53	137	1,32	3,18	433,5	703	4,139	0,015	0,27752	0,00072	0,74	1578,9	1662,1	1768,8	4,6	88
PFM001183B. Concordia upper intercept at 1843 ± 3 Ma, MSWD = 1,6 (with double error on 067/S.07 and 067/S.08)																		
057/S.61	T sb-fr b-rb tl (n=6)	6	41	70	2,87	1,74	13,3	681	5,247	0,031	0,33813	0,00169	0,85	1877,7	1860,3	1841,0	5,7	102
057/S.56 Reload	T eu-sb b-pb tl (n=38)	15	23	48	1,86	0,77	14,5	1035	5,147	0,021	0,33128	0,00107	0,77	1844,6	1843,9	1843,1	4,6	100
067/S.07	T eu pb tl (n=16)	11	28	64	1,80	0,81	11,7	1161	4,743	0,016	0,30446	0,00097	0,80	1713,4	1774,8	1847,9	3,7	92
067/S.08	T na fr pb tl (n=13)	6	27	70	1,90	0,80	7,2	938	3,943	0,018	0,25467	0,00109	0,79	1462,5	1622,6	1836,9	5,3	77
PFM002216A. Concordia upper intercept at 1886 ± 0,9 Ma, MSWD = 0,059																		
057/13	Z sb sp ts (n=5)	17	91	260	0,27	0,39	9,2	10199	5,395	0,016	0,33923	0,00092	0,97	1882,9	1884,1	1885,4	1,3	100
057/16	Z fr pb ts (n=1)	<1	>168	>500	0,28	1,24	3,4	3039	5,130	0,025	0,32366	0,00154	0,95	1807,6	1841,1	1879,2	2,8	96
057/18	Z sb sp ts (n=6)	2	210	605	0,25	0,72	3,6	7186	5,371	0,018	0,33778	0,00109	0,97	1876,0	1880,2	1884,9	1,4	99
057/17	Z fr ts (n=1)	47	83	239	0,25	0,05	4,5	52918	5,385	0,014	0,33858	0,00084	0,97	1879,9	1882,5	1885,4	1,1	100

[a] Omitted from the age calculation

[b] Z, Zircon; T, Titanite; na, non-abraded; eu, euhedral; sb, subhedral; an, anhedral; p, prismatic (l/w=3-4); sp, short prismatic (l/w=2); fr, fragment; b, brown; rb, red-brown; ob, olive-brown; pb, pale brown; ts, transparent; tl, transluscent; al, alt

[c] Weights and concentrations are known to better than 10%, except for zircon the weights of which were at, or below 1 µg, the limit of resolution of the balance

[d] Th/U model ratio inferred from $^{208}Pb/^{206}Pb$ ratio and age of sample

[e] Total common Pb in sample (initial + blank)

[f] Raw data corrected for fractionation and spike

[g] Corrected for fractionation, spike, blank and initial common Pb

[h] Uncertainty of $^{207}Pb/^{206}Pb$ age

[i] Degree of concordance; numbers >100 show reversed discordance

PFM000718G (U-Pb titanite)

Sample PFM000718G is from a Group D granite dyke from a coastal outcrop on Klubbudden that is situated northeast of the candidate area (Figure 1-2). As for PFM002210A, the granite dyke is strongly discordant to the intense tectonic banding in the surrounding rocks, defined primarily by different components of the Group B meta-intrusive rocks. It is also situated on the north-eastern limb of a major synform.

The upper intercept on the titanite concordia diagram (Figure 5-7), 1844±4 Ma, is interpreted as the age of cooling below the closure temperature of titanite, i.e. c 700-550°C /Frost et al, 2000/. The lower intercept, 909±200 Ma, suggests a Sveconorwegian lead-loss event for the titanites. One highly altered fraction, 067/S.03, has been omitted from the regression. The analysis point of this fraction is positioned far down and to the left on the concordia diagram, slightly below the discordia line. It has probably been affected by more than one lead-loss event, but is important in a qualitative sense since it confirms that the Sveconorwegian intercept is real.

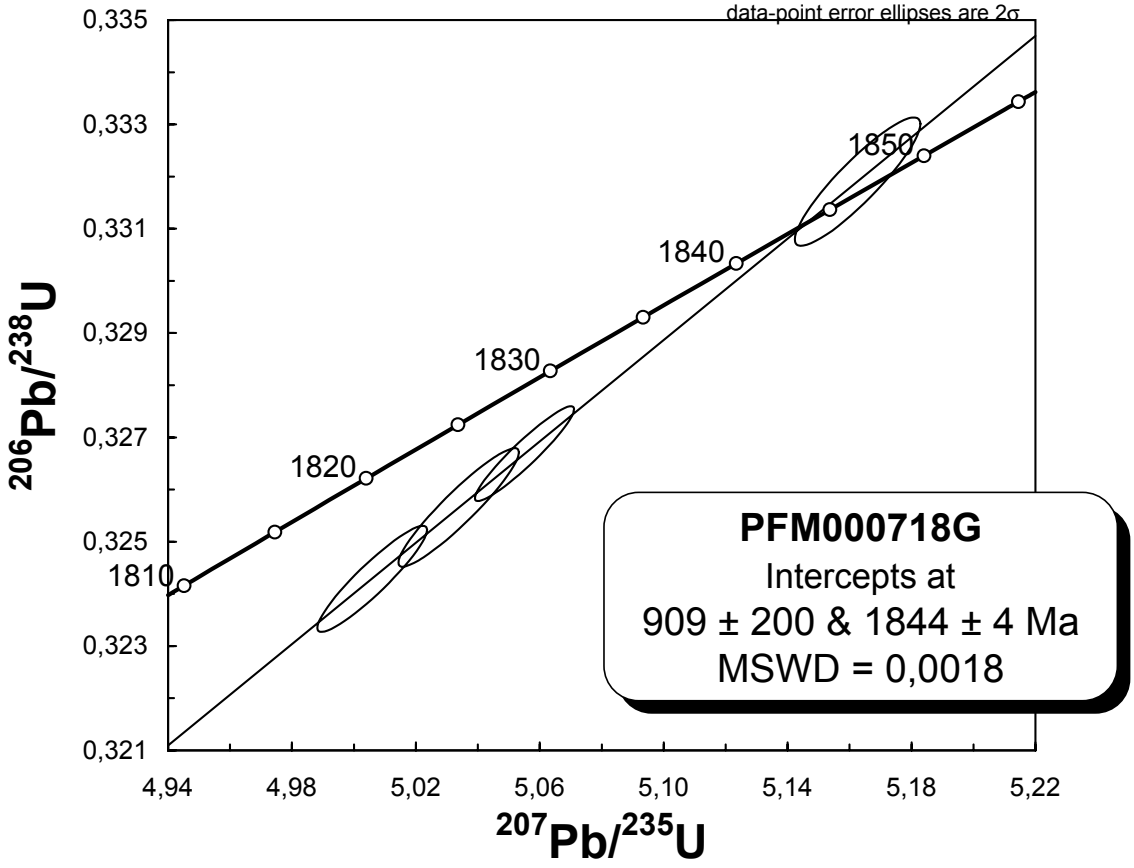

Figure 5-7. *Conventional concordia diagram for sample PFM000718G.*

PFM001183B (U-Pb titanite)

Sample PFM001183B is a Group B amphibolite from an outcrop outside yet close to the south-western margin of the candidate area (Figure 1-2). This sample is representative of the amphibolites that are intimately associated with the metagranite inside the candidate area. These amphibolites occur as dyke-like or irregular intrusive bodies inside the metagranite.

The upper intercept on the titanite concordia diagram (Figure 5-8), 1843±3 Ma, is interpreted as the age of cooling below the closure temperature of titanite, i.e. c 700–550°C /Frost et al, 2000/. It should be noted that the errors on the two discordant analyses have been doubled, since these two analyses are slightly aberrant and produce an unreasonably large error in the calculated age (1843±14 Ma). If one of the two analyses is omitted from the age calculation, the resulting age remains the same, but with a much lower error. Since there are neither analytical nor geological reasons to omit either of these analyses, the error has been doubled. This procedure gives rise to a better fit on the discordia line and a more reasonable error in the calculated age.

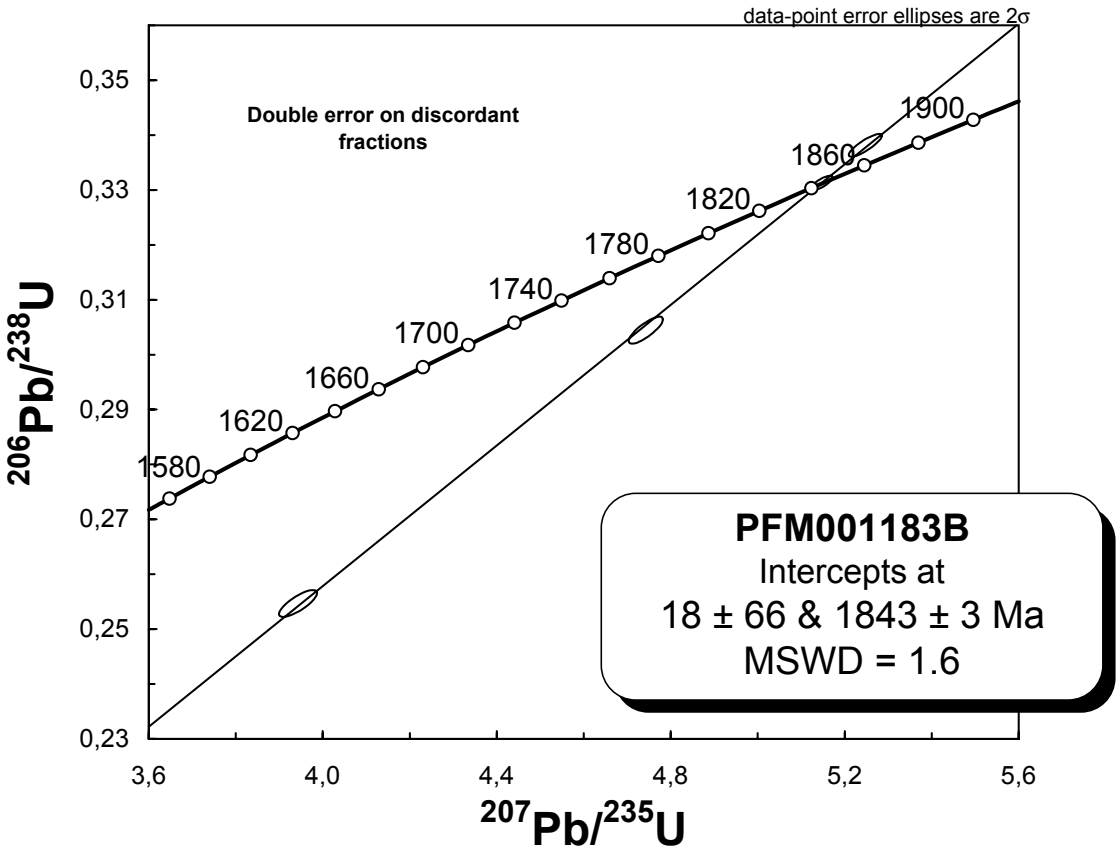

Figure 5-8. *Conventional concordia diagram for sample PFM001183B.*

PFM002216A (U-Pb zircon)

Sample PFM002216B is from a roadside outcrop in the southernmost part of one of the major Group B ultramafic to intermediate plutons that are situated west and south-west of the candidate area (Figure 1-2). On the basis of a geochemical analysis /Stephens et al, 2003b/, this sample is inferred to be gabbroic in composition.

The upper intercept on the zircon concordia diagram (Figure 5-9), 1886±0.9 Ma, is interpreted as the crystallisation age of this mafic to intermediate pluton.

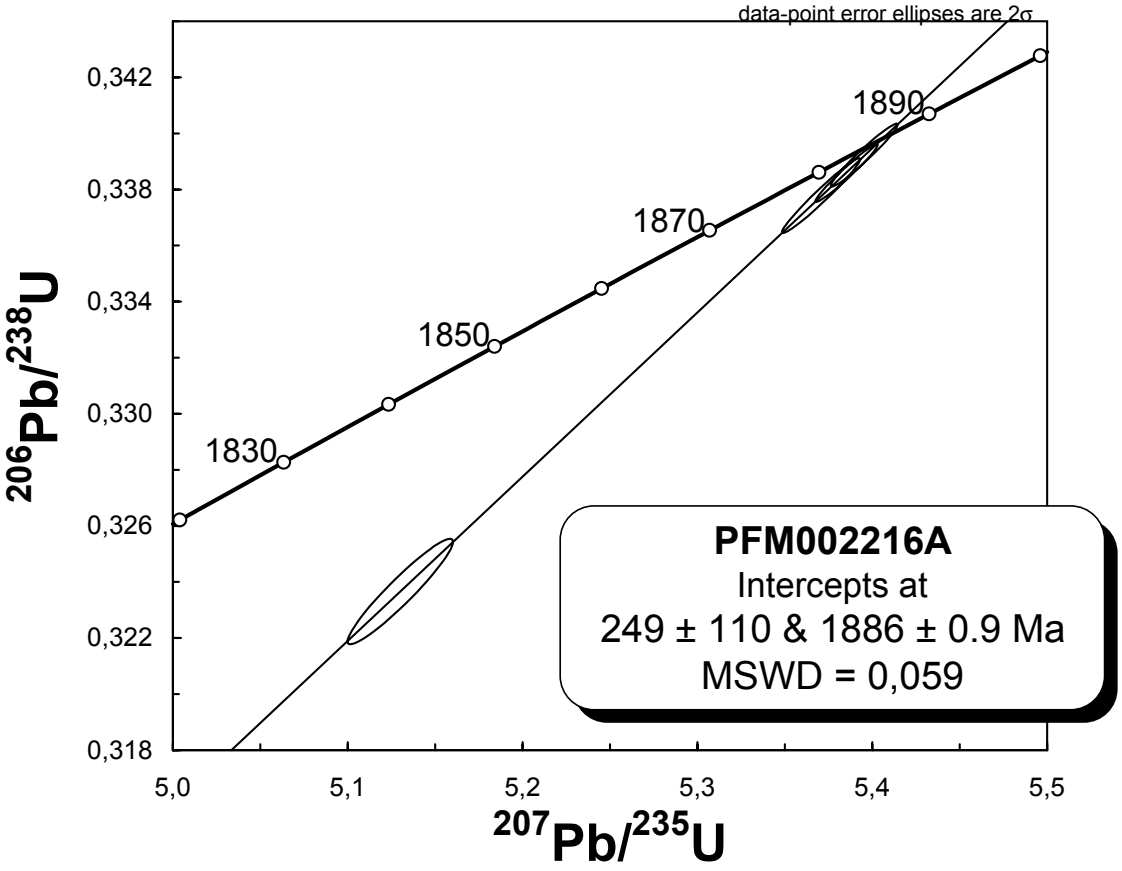

Figure 5-9. *Conventional concordia diagram for sample PFM002216A.*

5.2 $^{40}Ar/^{39}Ar$ hornblende ages

The $^{40}Ar/^{39}Ar$ hornblende data that have been used to calculate the nine ages presented here are listed in Table 5-3. All samples are from the surface.

Bearing in mind the calculated errors, the $^{40}Ar/^{39}Ar$ hornblende ages indicate cooling through c 500°C during the time interval 1834–1793 Ma. The four samples taken from the structural domains affected by more intense ductile deformation, to the north-east and to the southwest of the candidate area, yield consistently younger ages in the range 1812–1793 Ma. Both older ages in the range 1834–1819 Ma (three samples) and younger ages in the range 1807–1799 (two samples) are present in the candidate area, i.e. one of the structural domains that generally shows less intense ductile deformation. More data are required to confirm this disparity and to assess its geological significance.

A short summary of the results for each sample is presented below.

Table 5-3. $^{40}Ar/^{39}Ar$ hornblende data.

Sample/run ID[a]	Power (W)	Ca/K	Cl/K	$^{36}Ar/^{39}Ar$	$\%^{36}Ar(Ca)$[b]	$^{40}Ar^*/^{39}Ar$	^{39}Ar (Mol-14)	$\%^{39}Ar$[c]	Cum. $\%^{39}Ar$	$\%^{40}Ar^*$[d]	Age (Ma)	± 2σ
PFM002208A, run ID 1067-44 (J = 0.01071 ± 0.00001):												
1067-44A	2,3	5,26623	0,06283	0,028776	2,5	194,80	0,3515	5,1	5,1	95,9	2033,1	1,5
1067-44B	2,4	8,72945	0,04732	0,003755	32,0	168,28	0,8568	12,7	17,7	99,6	1859,0	1,0
•1067-44C	2,5	8,58089	0,04532	0,001816	65,1	163,58	1,7331	25,6	43,3	99,9	1826,3	1,6
•1067-44D	2,5	8,61668	0,04684	0,001592	74,6	163,76	2,0514	30,3	73,6	99,9	1827,5	0,9
•1067-44E	2,6	9,67932	0,04940	0,003314	40,2	164,04	0,1066	1,6	75,2	99,6	1829,5	2,3
•1067-44F	2,6	11,88924	0,09017	0,001400	117,0	159,00	0,0247	0,4	75,6	100,0	1793,8	27,1
•1067-44G	2,7	8,73560	0,05193	0,001972	61,0	163,94	0,6505	9,6	85,2	99,9	1828,8	1,9
•1067-44H	2,7	9,26881	0,05538	0,003520	36,3	163,77	0,0564	0,8	86,0	99,6	1827,6	3,7
•1067-44I	2,8	9,21709	0,04814	0,001950	65,1	163,73	0,4751	7,0	93,0	99,9	1827,3	1,2
•1067-44J	2,8	9,67641	0,04729	0,002349	56,8	163,72	0,2045	3,0	96,0	99,8	1827,3	1,7
•1067-44K	2,9	1,51354	0,04351	0,000988	21,1	158,24	0,0027	0,0	96,1	99,9	1788,4	38,0
1067-44L	3,1	9,50401	0,04295	0,001455	90,0	160,23	0,0781	1,2	97,2	100,0	1802,6	4,4
1067-44M	3,5	12,92285	0,09083	0,011284	15,8	159,94	0,0404	0,6	97,8	98,3	1800,5	7,8
1067-44N	5	10,78355	0,04797	0,002754	53,9	163,35	0,1473	2,2	100,0	99,8	1824,7	2,0
Integrated age=											1842	2
(•) Plateau age =								78,3			1828	2
PFM002209A, run ID 1054-45 (J = 0.01071 ± 0.00001):												
1054-45A	2,1	6,75235	0,02649	0,005015	18,5	150,50	0,4455	33,6	33,6	99,2	1732,1	1,5
•1054-45B	2,1	6,89992	0,02433	0,001338	71,0	159,29	0,5948	44,9	78,5	99,9	1795,9	1,3
•1054-45C	2,2	5,90505	0,00841	0,002811	28,9	160,12	0,0433	3,3	81,7	99,6	1801,8	4,4
•1054-45D	2,2	6,72082	0,02674	0,000665	139,2	159,33	0,1364	10,3	92,0	100,0	1796,2	2,3
•1054-45E	2,3	11,55939	0,14696	0,005626	28,3	158,90	0,0116	0,9	92,9	99,3	1793,1	14,2
•1054-45F	2,4	7,43254	0,03407	0,002260	45,3	159,00	0,0941	7,1	100,0	99,8	1793,8	3,6
Integrated age=											1775	3
(•) Plateau age =								66,4			1796	3
PFM002216A, run ID 1051-49 (J = 0.01071 ± 0.00001):												
1051-49A	2,1	36,56697	0,53023	3,834243	0,1	1350,16	0,0043	0,3	0,3	54,1	4940,1	29,8
1051-49B	2,3	15,97637	0,23863	0,014506	15,2	170,12	0,1595	10,6	10,8	97,9	1871,6	2,1
•1051-49C	2,4	15,28727	0,21729	0,003419	61,6	161,31	0,3451	22,9	33,7	99,8	1810,2	1,5
•1051-49D	2,4	15,01753	0,21376	0,003104	66,6	161,26	0,5109	33,8	67,5	99,8	1809,9	1,3
•1051-49E	2,4	15,19776	0,21645	0,002027	103,3	160,58	0,3744	24,8	92,3	100,0	1805,1	2,2
•1051-49F	2,5	18,58100	0,26252	0,006243	41,0	157,24	0,0170	1,1	93,5	99,3	1781,2	17,8
•1051-49H	2,8	15,10295	0,20101	0,000715	291,0	157,62	0,0988	6,5	100,0	100,3	1783,9	33,3
Integrated age=											1837	5
(•) Plateau age =								89,2			1809	3

PFM002219B, run ID 1058-52 (J = 0.01071 ± 0.00001):

1058-52A	1,7	22,44032	0,24539	0,727408	0,4	193,18	0,0067	0,8	0,8	47,2	2023,0	27,5
•1058-52B	1,9	10,12503	0,04052	0,002826	49,4	160,11	0,5724	66,6	67,4	99,7	1801,8	1,4
•1058-52C	2	9,87795	0,04569	0,001292	105,3	160,23	0,2246	26,1	93,5	100,0	1802,6	2,0
•1058-52E	3	12,15279	0,05515	0,001830	91,5	159,98	0,0542	6,5	100,0	100,0	1800,8	3,9
Integrated age=											1804	3
(•) Plateau age =								99,2			1802	3

PFM002239A, run ID 1057-54 (J = 0.01071 ± 0.00001):

1057-54A	1,7	6,92232	0,12400	0,145906	0,7	317,17	0,0573	5,1	5,1	88,1	2671,6	4,4
1057-54C	1,9	10,65382	0,11889	0,009617	15,3	160,00	0,0684	6,1	11,1	98,5	1801,0	2,3
1057-54D	1,9	3,59598	0,15344	0,002822	17,6	162,23	0,0105	0,9	12,1	99,6	1816,8	16,1
1057-54E	2	11,12666	0,11651	0,006369	24,1	169,21	0,3092	27,4	39,5	99,2	1865,4	1,5
•1057-54F	2	9,74614	0,10121	0,002960	45,4	160,41	0,4304	38,2	77,6	99,7	1803,9	1,6
•1057-54G	2,1	12,07526	0,01678	0,003493	47,6	159,41	0,0120	1,1	78,7	99,7	1796,7	15,3
•1057-54H	2,2	12,57148	0,12578	0,002020	85,7	158,37	0,0302	2,7	81,4	99,9	1789,3	7,2
•1057-54I	3	11,00766	0,10422	0,005121	29,6	160,91	0,2099	18,6	100,0	99,3	1807,4	2,2
Integrated age=											1876	3
(•) Plateau age =								60,5			1805	3

PFM002241A, run ID 1052-55 (J = 0.01071 ± 0.00001):

1052-55A	2,1	9,75633	0,60399	1,839127	0,1	2280,89	0,0146	0,3	0,3	80,7	5837,8	11,3
1052-55B	2,3	14,12438	0,05904	0,037888	5,1	164,17	0,0480	1,0	1,3	93,9	1830,4	3,7
1052-55C	2,4	16,37457	0,12505	0,041161	5,5	194,94	0,0308	0,7	2,0	94,4	2034,1	9,0
1052-55D	2,5	11,96792	0,04244	0,004019	41,0	168,06	1,2923	27,7	29,7	99,6	1857,4	1,0
•1052-55E	2,7	11,83282	0,04113	0,002296	71,0	164,18	2,8510	61,2	90,9	99,9	1830,5	1,4
•1052-55F	3,1	12,11468	0,04483	0,002634	63,4	164,40	0,4257	9,1	100,0	99,8	1832,0	2,2
Integrated age=											1885	3
(•) Plateau age =								70,3			1831	3

PFM002242A, run ID 1053-57 (J = 0.01071 ± 0.00001):

1053-57A	2,1	13,47117	0,19414	0,186340	1,0	393,49	0,1359	1,9	1,9	87,8	2979,3	2,8
•1053-57B	2,3	7,91648	0,12091	0,002801	38,9	163,23	1,2492	17,2	19,1	99,7	1823,8	1,0
•1053-57C	2,4	7,86804	0,12369	0,003038	35,7	162,66	0,1285	1,8	20,9	99,6	1819,8	2,2
•1053-57D	2,4	7,35210	0,12239	0,001752	57,8	162,63	2,2006	30,3	51,2	99,9	1819,6	1,2
•1053-57E	2,4	7,28640	0,12282	0,001562	64,3	162,80	1,2135	16,7	67,9	99,9	1820,8	1,0
•1053-57F	2,5	7,32106	0,12351	0,001824	55,3	162,77	1,7215	23,7	91,6	99,9	1820,6	1,0
1053-57G	2,5	7,57575	0,12321	0,001207	86,4	162,28	0,2998	4,1	95,8	100,0	1817,2	1,7
1053-57H	2,5	7,81443	0,13208	0,003014	35,7	162,22	0,2571	3,5	99,3	99,7	1816,7	1,6
1053-57I	2,6	7,38304	0,13505	0,007613	13,4	159,59	0,0495	0,7	100,0	98,8	1798,0	4,4
Integrated age=											1851	2
(•) Plateau age =								89,8			1821	2

PFM002244A, run ID 1056-59 (J = 0.01071 ± 0.00001):

1056-59A	1,9	5,87725	0,07516	0,007326	11,1	165,43	0,7645	43,2	43,2	98,8	1839,2	1,1
•1056-59B	1,9	6,08697	0,08334	0,001373	61,1	160,67	0,4706	26,6	69,8	99,9	1805,7	1,2
•1056-59C	2	6,18787	0,08202	0,001116	76,4	159,71	0,1052	5,9	75,8	100,0	1798,9	2,5
•1056-59D	2	5,72579	0,09115	0,000186	423,5	160,23	0,0625	3,5	79,3	100,1	1802,6	3,1
•1056-59F	2,2	7,89316	0,12271	0,009005	12,1	158,11	0,0294	1,7	81,0	98,5	1787,4	8,2
•1056-59G	2,7	6,16955	0,08084	0,001381	61,6	160,55	0,3362	19,0	100,0	99,9	1804,9	1,5
Integrated age=											1819	3
(•) Plateau age =								56,8			1804	3

PFM002245A, run ID 1055-61 (J = 0.01071 ± 0.00001):

1055-61A	1,8	14,67125	0,41780	0,420131	0,5	402,49	0,0060	0,4	0,4	76,4	3012,3	28,1
1055-61B	1,9	8,91066	0,07674	0,004255	28,8	156,04	0,0809	5,6	6,0	99,4	1772,6	3,3
•1055-61C	2	8,80101	0,07617	0,001917	63,2	160,98	0,6053	42,0	48,1	99,9	1807,9	1,2
•1055-61D	2	8,73942	0,07199	0,001574	76,5	161,03	0,4553	31,6	79,7	99,9	1808,3	1,5
•1055-61E	2	9,51756	0,08207	0,003713	35,3	160,92	0,0659	4,6	84,3	99,6	1807,5	2,9
•1055-61F	2,1	12,09834	0,08823	0,010611	15,7	160,41	0,0232	1,6	85,9	98,4	1803,9	9,3
•1055-61G	2,2	8,76094	0,08071	0,000824	146,5	160,41	0,0912	6,3	92,2	100,1	1803,8	2,9
•1055-61H	2,3	9,70198	0,05755	0,002818	47,4	160,67	0,0466	3,2	95,5	99,7	1805,7	4,1
1055-61I	2,4	11,43990	0,11531	0,005511	28,6	153,63	0,0101	0,7	96,2	99,2	1755,1	12,8
1055-61J	2,5	8,57507	0,08619	0,000103	1146,9	159,63	0,0548	3,8	100,0	100,2	1798,4	3,3
Integrated age=											1812	3
(•) Plateau age =								89,4			1808	3

a • Indicates steps included in the plateau age. Integrated age = the age calculated from all steps analysed; (•) Plateau age = the age calculated from steps that constitute a plateau, i.e. the interpreted true age of the sample

b Percentage of the total ^{36}Ar that is produced from Ca during irradiation (used to correct for atmospheric ^{40}Ar)

c Percentage ^{39}Ar released during each step

d Percentage of measured ^{40}Ar that is radiogenic

PFM002208A

Sample PFM002208A is a Group B amphibolite that is spatially associated with medium-grained metagranite inside the candidate area (Figure 1-2). The sampling locality lies within the structural domain that generally shows less intense ductile deformation. It is also situated in the bedrock block between the Eckarfjärden and Singö deformation zones (Figure 1-2).

The plateau age defined on the $^{40}Ar/^{39}Ar$ step-heating spectrum diagram is 1828±2 Ma (Figure 5-10). The age is interpreted as the age of cooling below the closure temperature of hornblende (c 500°C).

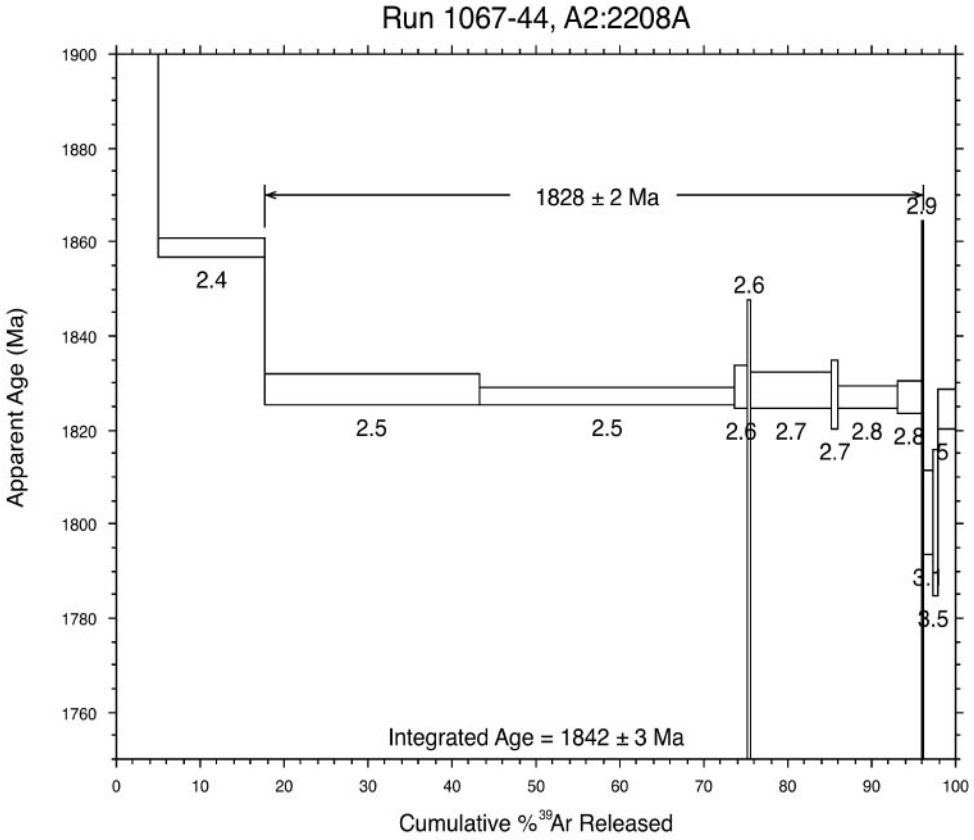

Figure 5-10. *$^{40}Ar/^{39}Ar$ hornblende step-heating spectrum for sample PFM002208A.*

PFM002209A

Sample PFM002209A is a Group B amphibolite that is spatially associated with aplitic metagranite along the coast at Klubbudden (Figure 1-2). The sampling locality lies within the structural domain that shows more intense ductile deformation to the north-east of the candidate area. It is also situated in the bedrock block between the Eckarfjärden and Singö deformation zones, relatively close to the Singö deformation zone (Figure 1-2).

The plateau age defined on the $^{40}Ar/^{39}Ar$ step-heating spectrum diagram is 1796±3 Ma (Figure 5-11). The age is interpreted as the age of cooling below the closure temperature of hornblende (c 500°C).

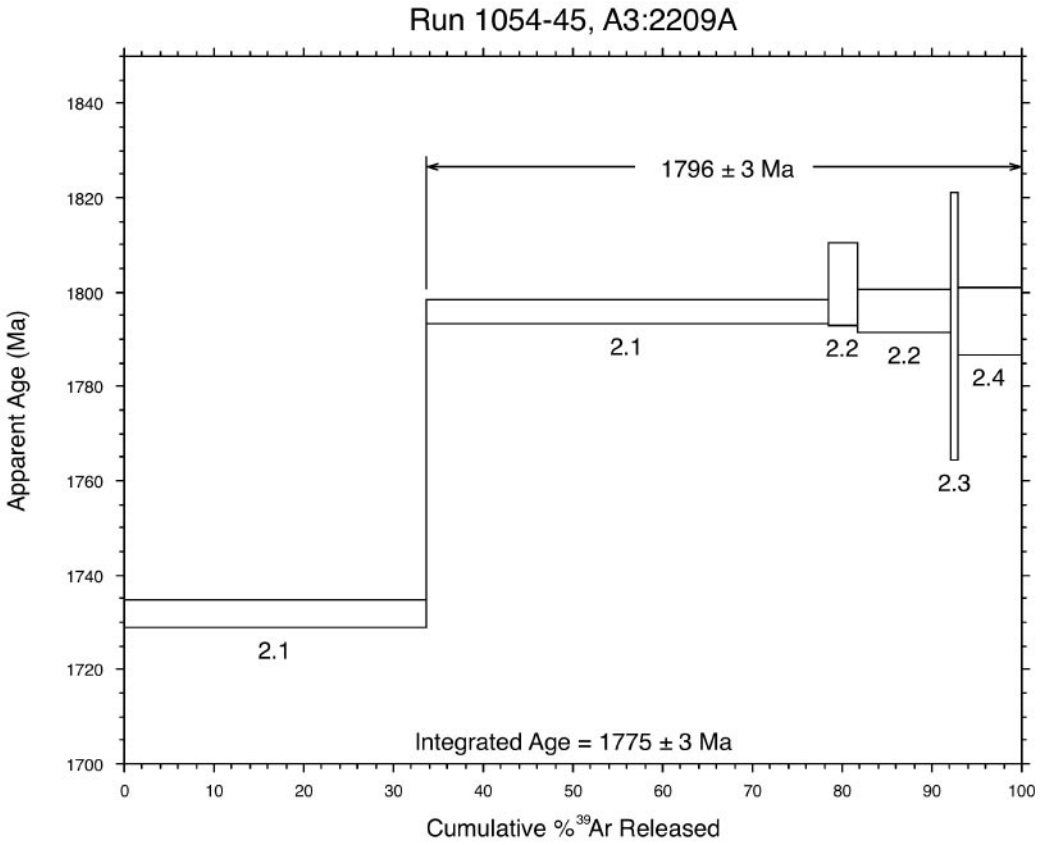

Figure 5-11. *$^{40}Ar/^{39}Ar$ hornblende step-heating spectrum for sample PFM002209A.*

PFM002216A

Sample PFM002216A is a Group B metagabbro. The sampling locality is a roadside outcrop in the southernmost part of one of the major Group B ultramafic to intermediate plutons that are situated west and south-west of the candidate area (Figure 1-2). On the basis of a geochemical analysis /Stephens et al, 2003b/, this sample is inferred to be gabbroic in composition. The locality lies within the structural domain that shows more intense ductile deformation to the south-west of the candidate area. It is also situated in the bedrock block between the Eckarfjärden and Singö deformation zones, relatively close to the Eckarfjärden deformation zone (Figure 1-2).

The plateau age defined on the $^{40}Ar/^{39}Ar$ step-heating spectrum diagram is 1809±3 Ma (Figure 5-12). The age is interpreted as the age of cooling below the closure temperature of hornblende (c 500°C).

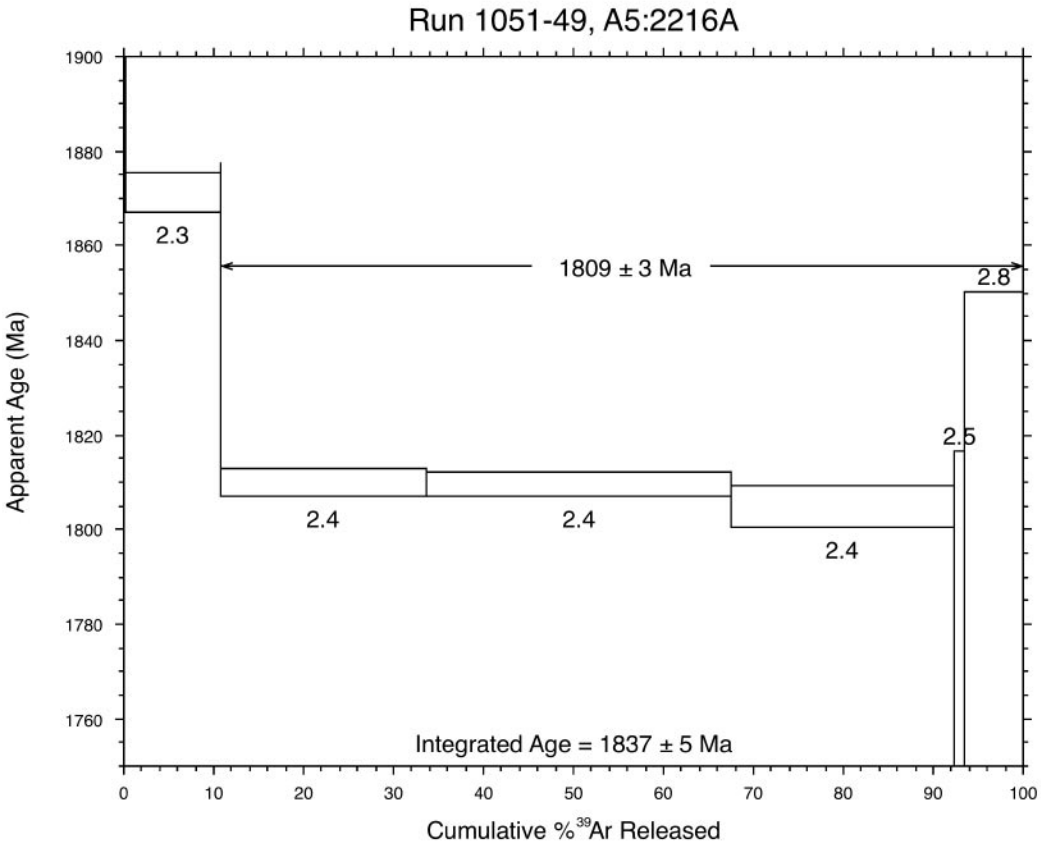

Figure 5-12. *$^{40}Ar/^{39}Ar$ hornblende step-heating spectrum for sample PFM002216A.*

PFM002219B

Sample PFM002219B is a Group B amphibolite. The sampling locality is a small roadside outcrop that is situated close to drill site 1, inside yet close to the south-western margin of the candidate area (Figure 1-2). It is spatially associated with medium-grained metagranite to metagranodiorite. The locality lies within the structural domain that generally shows less intense ductile deformation. However, the degree of ductile deformation, with the development of a distinctive, planar grain-shape fabric, increases towards the margin of the granite pluton. The sampling locality is also situated in the bedrock block between the Eckarfjärden and Singö deformation zones (Figure 1-2).

The plateau age defined on the $^{40}Ar/^{39}Ar$ step-heating spectrum diagram is 1802±3 Ma (Figure 5-13). The age is interpreted as the age of cooling below the closure temperature of hornblende (c 500°C).

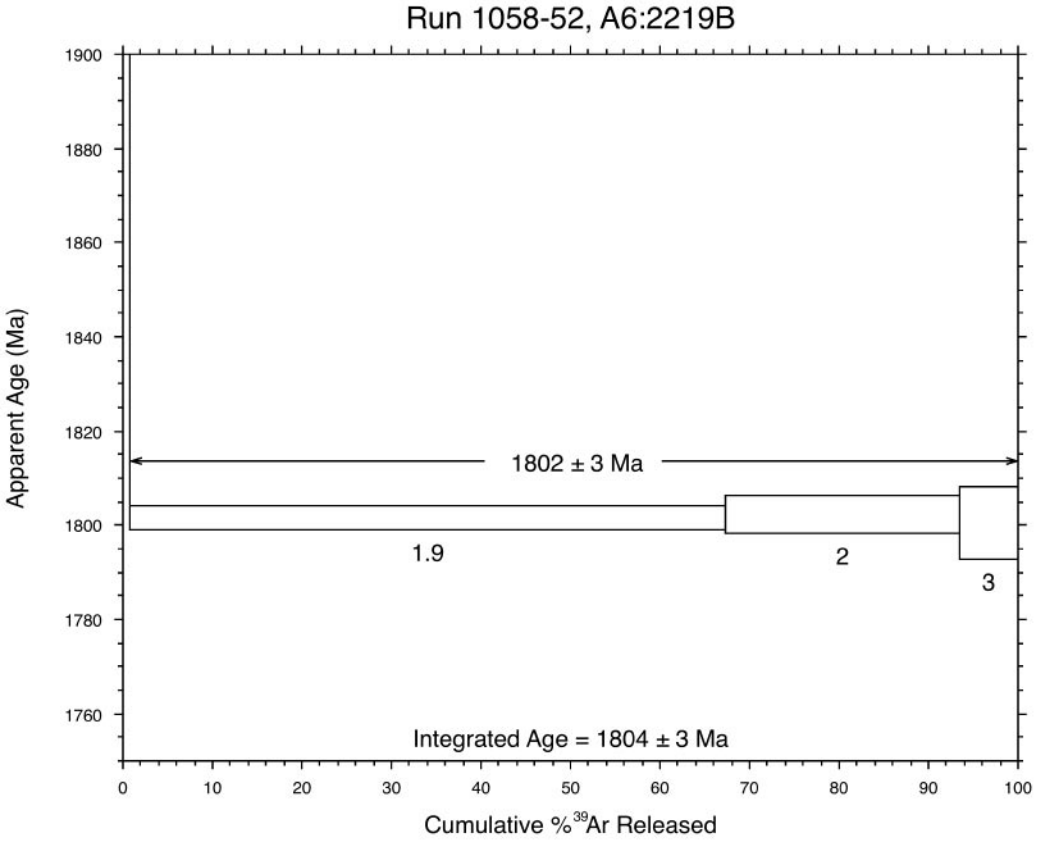

Figure 5-13. *$^{40}Ar/^{39}Ar$ hornblende step-heating spectrum for sample PFM002219B.*

PFM002239A

Sample PFM002239A is a Group B amphibolite that is spatially associated with metatonalite to the west of the candidate area (Figure 1-2). The locality lies within the structural domain that shows more intense ductile deformation. It is also situated close to the Forsmark deformation zone (Figure 1-2).

The plateau age defined on the $^{40}Ar/^{39}Ar$ step-heating spectrum diagram is 1805±3 Ma, (Figure 5-14). The age is interpreted as the age of cooling below the closure temperature of hornblende (c 500°C).

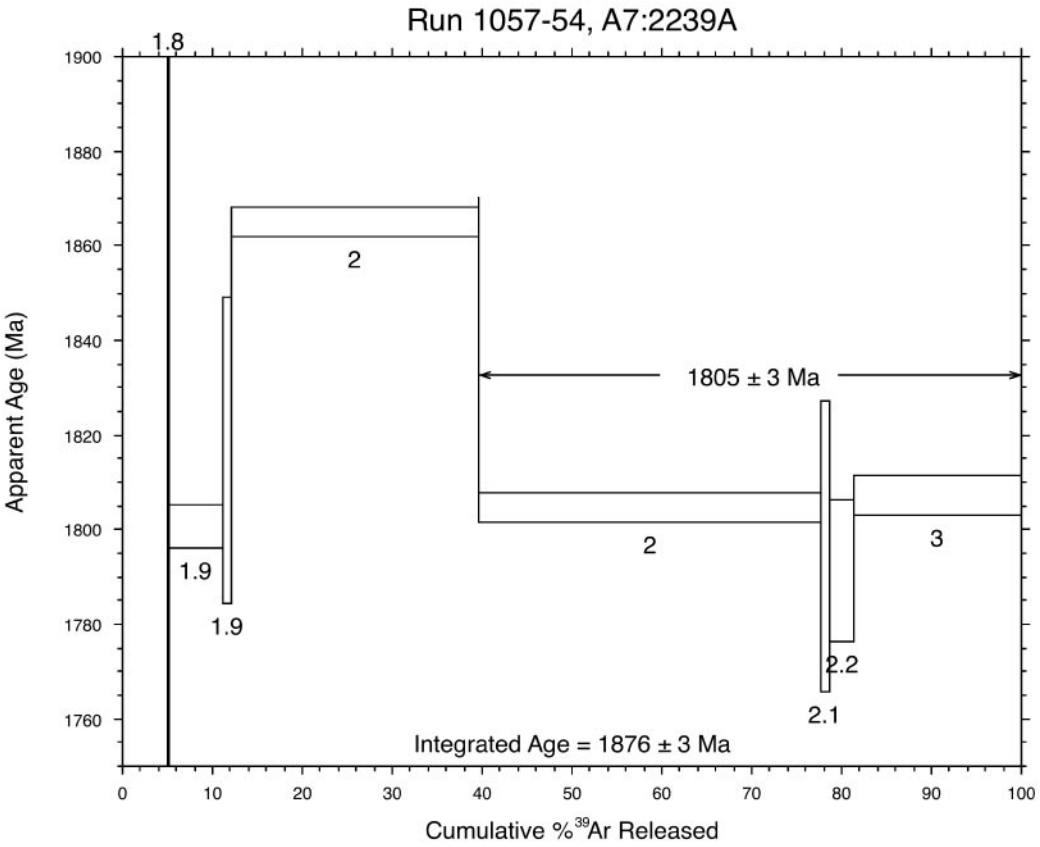

Figure 5-14. *$^{40}Ar/^{39}Ar$ hornblende step-heating spectrum for sample PFM002239A.*

PFM002241A

Sample PFM002241A is a Group B amphibolite from drill site 3 (Figure 1-2). It is spatially associated with pegmatitic granite and medium-grained metagranite. The locality lies within the structural domain that generally shows less intense ductile deformation. The sampling locality is also situated in the bedrock block between the Eckarfjärden and Singö deformation zones (Figure 1-2).

The age obtained, 1831±3 Ma, consists of only two steps and does not constitute a true plateau (Figure 5-15). However, this age is consistent with other ages in the area and, for this reason, it is considered as relevant. The age is interpreted as dating the cooling below the closure temperature of hornblende (c 500°C).

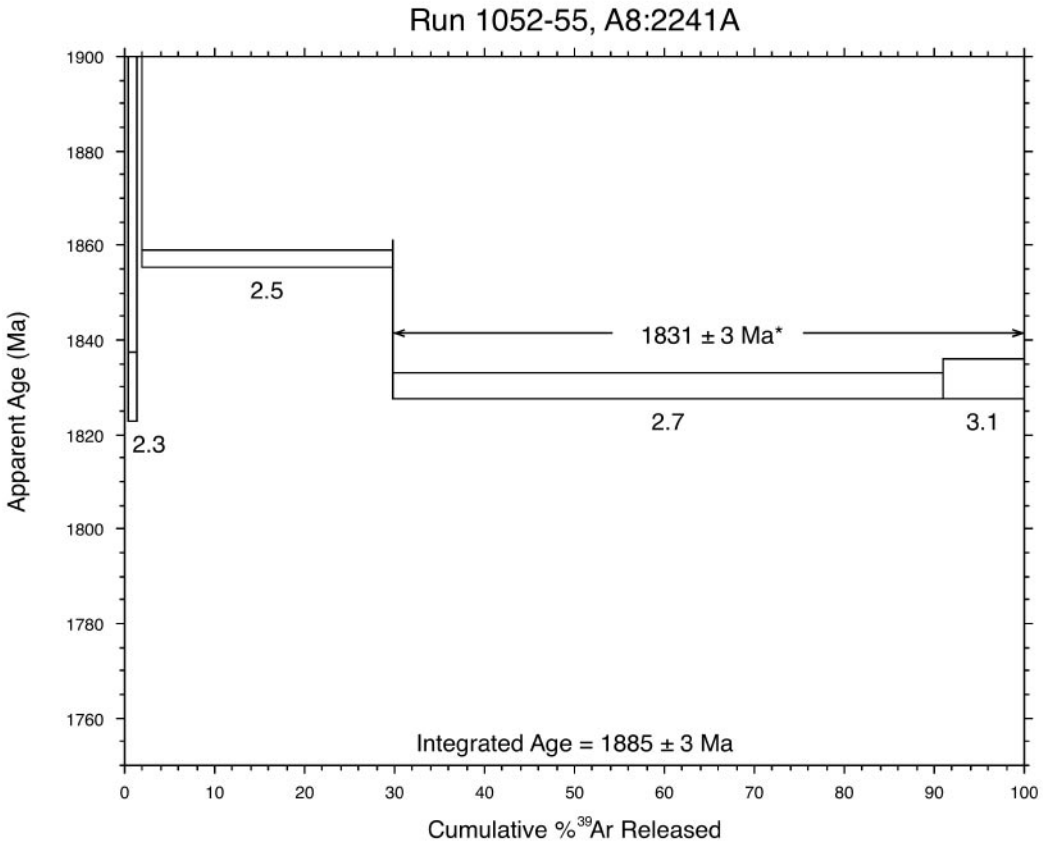

Figure 5-15. *$^{40}Ar/^{39}Ar$ hornblende step-heating spectrum for sample PFM002241A. The asterisk indicates that there are only two steps and that there is no true plateau according to the criteria used here /Dalrymple and Lamphere, 1971/.*

PFM002242A

Sample PFM002242A is a Group B amphibolite that is situated within yet close to the north-eastern margin of the candidate area (Figure 1-2). It is spatially associated with medium-grained metagranite. The locality lies within the structural domain that generally shows less intense ductile deformation. The sampling locality is also situated in the bedrock block between the Eckarfjärden and Singö deformation zones (Figure 1-2).

The plateau age defined on the $^{40}Ar/^{39}Ar$ step-heating spectrum diagram is 1821±2 Ma (Figure 5-16). The age is interpreted as the age of cooling below the closure temperature of hornblende (c 500°C).

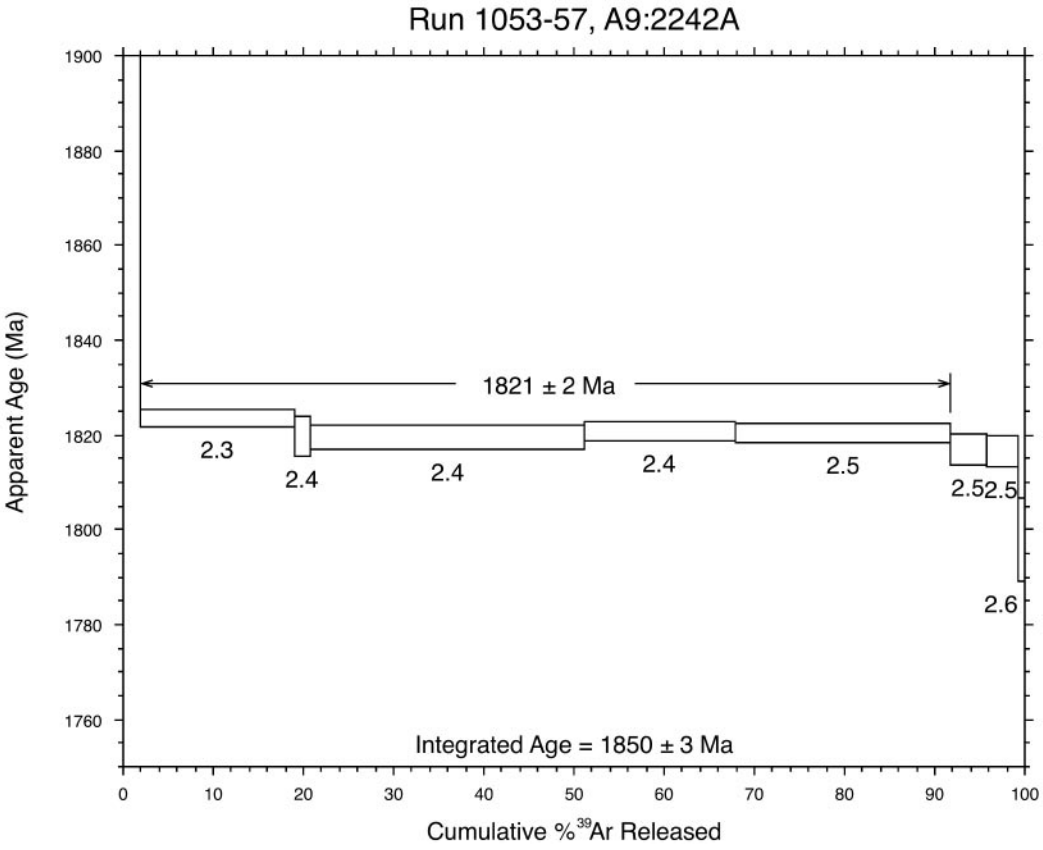

Figure 5-16. *$^{40}Ar/^{39}Ar$ hornblende step-heating spectrum for sample PFM002242A.*

PFM002244A

Sample PFM002244A is a Group B amphibolite that is situated south of drill site 2 in the candidate area and is spatially associated with medium-grained metagranite (Figure 1-2). The locality lies within the structural domain that generally shows less intense ductile deformation. The sampling locality is also situated in the bedrock block between the Eckarfjärden and Singö deformation zones (Figure 1-2).

The plateau age defined on the $^{40}Ar/^{39}Ar$ step-heating spectrum diagram is 1804±3 Ma, (Figure 5-17). The age is interpreted as the age of cooling below the closure temperature of hornblende (c 500°C).

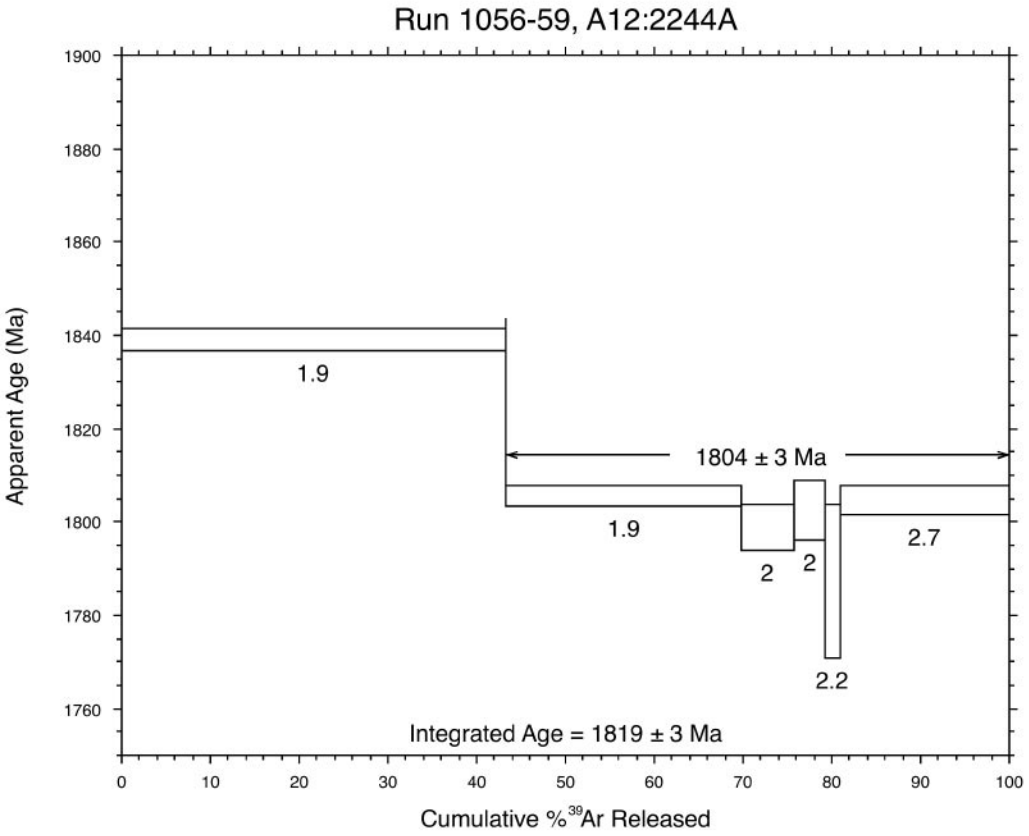

Figure 5-17. *$^{40}Ar/^{39}Ar$ hornblende step-heating spectrum for sample PFM002244A.*

PFM002245A

Sample PFM002245A is a Group B amphibolite that is situated north-west of the lake Eckarfjärden (Figure 1-2). It is spatially associated with metagranite similar to that observed inside the candidate area. The locality lies within the structural domain that shows more intense ductile deformation. The sampling locality is also situated close to the Eckarfjärden deformation zone (Figure 1-2).

The plateau age defined on the $^{40}Ar/^{39}Ar$ step-heating spectrum diagram is 1808±3 Ma (Figure 5-18). The age is interpreted as the age of cooling below the closure temperature of hornblende (c 500°C).

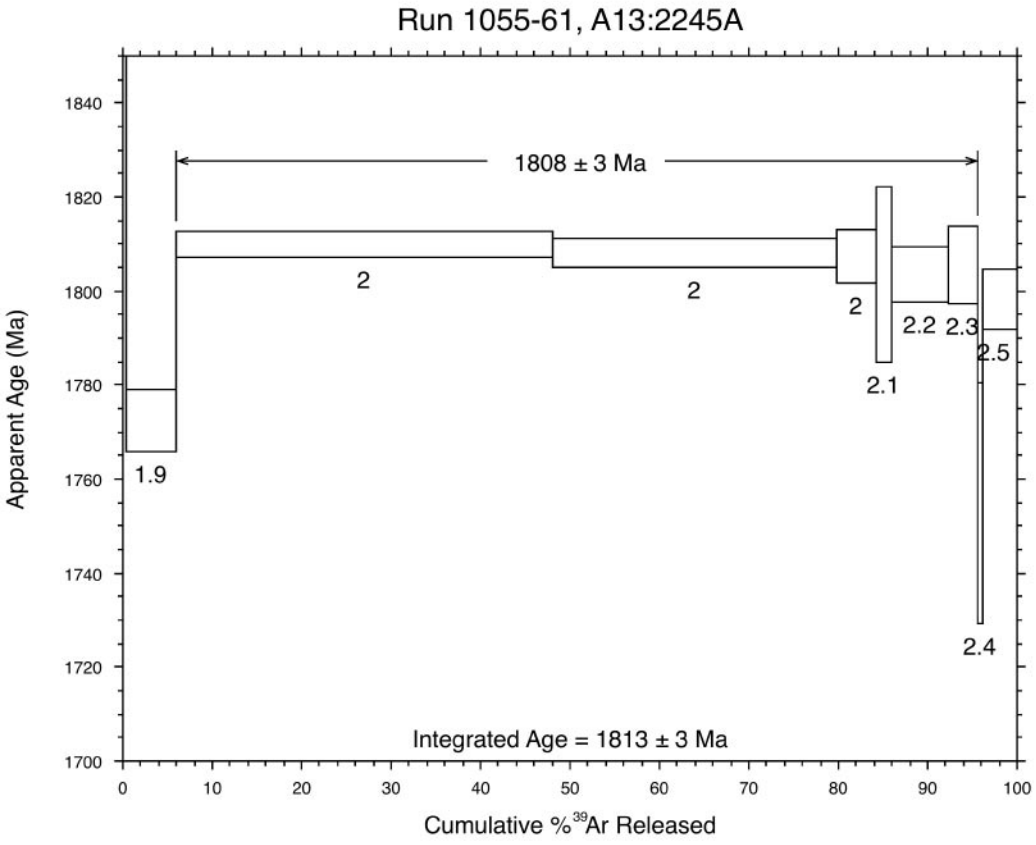

Figure 5-18. *$^{40}Ar/^{39}Ar$ hornblende step-heating spectrum for sample PFM002245A.*

5.3 $^{40}Ar/^{39}Ar$ biotite ages

The $^{40}Ar/^{39}Ar$ biotite data that have been used to calculate the eight ages presented here are listed in Table 5-4. These include six age determinations from surface samples and two age determinations from samples taken from borehole KFM01A.

Bearing in mind the calculated errors, the ages obtained from the surface samples and from the upper part of KFM01A indicate cooling through 300°C between 1704 Ma and 1666 Ma. An age of 1639±4 Ma has been obtained from the sample at the bottom of KFM01A (c 1000 m). This result is consistent with the fact that deeper levels of the crust will pass through the 300° isotherm at a later stage than shallower levels. An uplift rate of c 25 m/Ma after 1643 Ma is indicated from the $^{40}Ar/^{39}Ar$ biotite data from borehole KFM01A. For comparison purposes, it may be noted that the present rate of uplift in northern Uppland, following the latest glaciation, is 6000 m/Ma.

The variation in the ages of the surface samples may reflect different crustal levels that have been offset, with respect to each other, by faulting after c 1671 Ma. The oldest $^{40}Ar/^{39}Ar$ biotite ages come from samples PFM000875A and PFM001240A. These samples are situated within the bedrock block between the Eckarfjärden and Forsmark deformation zones and the bedrock block to the southwest of the Forsmark deformation zone, respectively. More data are required to investigate the geological significance of the variation in the ages of the surface samples.

A short summary of the results for each sample is presented below.

Table 5-4. $^{40}Ar/^{39}Ar$ biotite data.

Sample/Run Id[a]	Power (W)	Ca/K	Cl/K	$^{36}Ar/^{39}Ar$	$\%^{36}Ar(Ca)$[b]	$^{40}Ar^*/^{39}Ar$	^{39}Ar (Mol-14)	$\%^{39}Ar$[c]	Cum. $\%^{39}Ar$	$\%^{40}Ar^*$[d]	Age (Ma)	± 1σ
PFM000256A, Run ID 1155-01 (J = 0.01041 ± 0.00004):												
1155-01A	1,2	0,14117	0,03806	0,020969	0,1	66,57625	0,046	1,8	1,8	91,5	949,91304	3,08487
1155-01B	1,3	0,02035	0,02256	0,006821	0	140,20686	0,1604	5,7	7,5	98,6	1623,63301	1,57139
1155-01C	1,3	0,01536	0,02234	0,002249	0,1	144,60047	0,198	7,1	14,5	99,5	1656,87326	1,62701
•1155-01D	1,4	0,01758	0,02521	0,001621	0,1	146,74463	0,2805	10	24,6	99,7	1672,87535	1,49771
•1155-01E	1,4	0,00649	0,0248	0,00071	0,1	146,15152	0,2509	8,9	33,5	99,9	1668,46308	1,91449
•1155-01F	1,4	0,0124	0,02707	0,000836	0,2	146,57889	0,1915	6,8	40,3	99,8	1671,64347	1,89147
•1155-01G	1,5	0,02431	0,02376	0,000773	0,4	146,12545	0,1533	5,5	45,8	99,8	1668,26891	2,24085
•1155-01H	1,5	0,02033	0,02586	0,000148	1,9	146,81996	0,1146	4,1	49,9	100	1673,43503	2,26912
•1155-01I	1,6	0,01821	0,02502	0,000616	0,4	146,7849	0,1974	7	56,9	99,9	1673,17454	1,75284
•1155-01J	1,8	0,01702	0,02436	0,000855	0,3	146,79064	0,3378	12	68,9	99,8	1673,21717	1,1313
•1155-01K	2,3	0,01215	0,02286	0,000675	0,2	146,13768	0,6243	22,2	91,1	99,9	1668,36002	1,34159
1155-01L	2,5	0,04371	0,03591	0,001231	0,5	145,52522	0,0756	2,7	93,8	99,8	1663,79216	2,46984
1155-01M	3,5	0,01493	0,0237	0,001152	0,2	146,29735	0,1737	6,2	100	99,8	1669,54895	1,54839
Integrated age =											1656	4
(•) Plateau age =							76,6				1671	5
PFM000875A, Run ID 1151-01 (J = 0.01041 ± 0.00004):												
1151-01A	1,3	0,11052	0,07862	0,03533	0	125,48329	0,0074	0,2	0,2	92,3	1507,5524	17,90929
1151-01B	1,3	0,04745	0,05429	0,01416	0	123,19525	0,0655	1,6	1,9	96,7	1488,82363	3,11953
1151-01C	1,4	0,02691	0,05464	0,002073	0,2	144,88261	0,3461	8,7	10,5	99,6	1658,98701	1,27705
•1151-01D	1,4	0,03173	0,05157	0,000665	0,6	150,43929	1,1791	29,7	40,2	99,9	1700,12034	1,11684
•1151-01E	1,5	0,07312	0,05349	0,000529	1,9	150,62332	0,3454	8,7	48,9	99,9	1701,46675	1,20151
•1151-01F	1,5	0,04647	0,05197	0,000489	1,3	150,63418	0,5004	12,6	61,5	99,9	1701,54615	1,06754
•1151-01G	1,6	0,10677	0,06184	0,001319	1,1	150,10659	0,0593	1,5	63	99,7	1697,68378	2,96028
•1151-01H	1,7	0,24036	0,0557	0,000145	22,4	150,25857	0,1042	2,6	65,6	100	1698,79727	2,24554
•1151-01I	1,9	0,11331	0,04942	0,000434	3,5	150,29839	0,602	15,2	80,8	99,9	1699,08889	1,29323
1151-01J	2,1	0,2516	0,05091	0,000653	5,2	149,70998	0,4261	10,8	91,6	99,9	1694,77483	1,76188
1151-01K	2,3	0,40784	0,05582	0,000896	6,1	149,8277	0,2205	5,6	97,1	99,8	1695,6387	2,01587
1151-01L	2,7	1,86356	0,05986	0,00168	14,9	151,6853	0,1141	2,9	100	99,7	1709,21666	4,18589
Integrated age =											1692	4
(•) Plateau age =							70,3				1700	4

PFM001240A, Run ID 1156-01 (J = 0.01041 ± 0.00004):

1156-01A	1,2	0,46257	0,06343	0,027125	0,2	66,05639	0,0459	0,9	0,9	89,2	944,13724	3,26447
1156-01B	1,3	0,0826	0,04845	0,007414	0,2	112,86569	0,1445	2,5	3,4	98,1	1401,76315	2,0029
1156-01C	1,3	0,03913	0,05329	0,003627	0,1	137,19629	0,1135	2	5,3	99,2	1600,49745	1,98658
1156-01D	1,4	0,01866	0,05274	0,002729	0,1	140,69223	0,2352	4,1	9,4	99,4	1627,33541	2,04753
1156-01E	1,4	0,01549	0,05167	0,000827	0,3	147,34608	0,2848	5	14,3	99,8	1677,33867	1,63272
1156-01F	1,4	0,01154	0,05094	0,000721	0,2	148,37054	0,3112	5,4	19,7	99,9	1684,91584	1,2553
1156-01G	1,5	0,02191	0,05341	0,000917	0,3	149,17692	0,3515	6,1	25,9	99,8	1690,85768	1,64185
1156-01H	1,5	0,01282	0,05087	0,000576	0,3	149,26656	0,3847	6,7	32,5	99,9	1691,51695	1,33085
1156-01I	1,5	0,01321	0,04979	0,000724	0,2	149,70042	0,3521	6,1	38,6	99,9	1694,70466	1,10794
•1156-01J	1,7	0,03593	0,04972	0,000689	0,7	150,41199	0,5813	10,1	48,7	99,9	1699,92054	1,04105
•1156-01K	1,9	0,08607	0,05064	0,000475	2,4	150,604	0,942	16,3	65	99,9	1701,32546	2,07735
•1156-01L	2,1	0,11836	0,0497	0,000576	2,8	150,32478	0,7362	12,8	77,8	99,9	1699,28208	1,18517
•1156-01M	2,4	0,1061	0,04904	0,000323	4,4	150,26728	0,8672	15,1	92,9	99,9	1698,86101	1,25826
•1156-01N	2,8	0,08141	0,05073	0,000397	2,8	150,1575	0,4099	7,1	100	99,9	1698,05683	1,31661
Integrated age =											1679	4
(•) Plateau age =								61,4			1699	4

PFM002207A, Run ID 1157-01 (J = 0.01041 ± 0.00004):

1157-01A	1,3	0,01494	0,0472	0,013853	0	100,89665	0,2192	2	2	96,1	1295,33246	1,39369
1157-01B	1,3	0,01061	0,04994	0,004846	0	116,30585	0,2884	2,6	4,6	98,8	1431,22692	1,43993
1157-01C	1,4	0,00855	0,04868	0,001885	0,1	140,7186	0,7135	6,4	11	99,6	1627,53628	1,17431
1157-01D	1,4	0,00635	0,03121	0,001297	0,1	143,8974	0,8506	7,6	18,6	99,7	1651,59509	1,35822
1157-01E	1,5	0,01003	0,05005	0,000903	0,1	145,7449	0,7086	6,4	25	99,8	1665,43191	1,07184
1157-01F	1,5	0,00753	0,04904	0,000527	0,2	146,02331	1,044	9,4	34,4	99,9	1667,50795	1,21796
1157-01G	1,5	0,00944	0,04947	0,00061	0,2	146,03613	0,7955	7,1	41,5	99,9	1667,60346	1,04574
1157-01H	1,6	0,00525	0,04894	0,000578	0,1	146,41712	0,8368	7,5	49	99,9	1670,44033	1,05324
1157-01I	1,7	0,00778	0,04839	0,000607	0,2	146,93335	0,8622	7,7	56,8	99,9	1674,27703	1,107
•1157-01J	1,8	0,00778	0,04932	0,00097	0,1	147,76329	0,7413	6,7	63,4	99,8	1680,42832	1,07647
•1157-01K	1,9	0,00876	0,04904	0,000815	0,1	147,6488	0,8799	7,9	71,3	99,8	1679,581	2,22665
•1157-01L	2,1	0,00937	0,04979	0,000849	0,1	147,76639	1,1753	10,5	81,8	99,8	1680,45123	1,24556
•1157-01M	2,3	0,00892	0,04794	0,000623	0,2	147,54255	1,3479	12,1	93,9	99,9	1678,79434	1,16389
•1157-01N	2,5	0,01299	0,04987	0,000644	0,3	147,39237	0,2092	1,9	95,8	99,9	1677,68174	1,84947
1157-01O	2,8	0,08263	0,03335	0,000562	2	147,04577	0,4686	4,2	100	99,9	1675,11152	1,32795
Integrated age =											1657	4
(•) Plateau age =								39			1680	4

PFM002213A, Run ID 1152-01 (J = 0.01041 ± 0.00004):

1152-01A	1,3	0,07651	0,03574	0,019418	0,1	106,6443	0,1612	2,7	2,7	94,9	1347,22564	1,76658
1152-01B	1,4	0,03117	0,03395	0,002962	0,1	135,58634	0,2354	4	6,7	99,4	1588,00252	1,8168
1152-01C	1,4	0,02485	0,03399	0,001467	0,2	143,07389	0,3702	6,2	13	99,7	1645,3931	1,33654
1152-01D	1,4	0,01359	0,02946	0,00077	0,2	145,00476	0,4334	7,3	20,3	99,8	1659,90143	1,15487
•1152-01E	1,5	0,01446	0,02971	0,000377	0,5	146,49244	1,623	27,4	47,7	99,9	1671,00064	1,5133
•1152-01F	1,5	0,01632	0,03279	0,000643	0,3	146,59281	0,3317	5,6	53,3	99,9	1671,74702	1,49423
•1152-01G	1,6	0,02149	0,0334	0,00092	0,3	146,94716	0,1671	2,8	56,1	99,8	1674,37961	1,67024
•1152-01H	1,7	0,02251	0,02947	0,00029	1	146,84969	0,6787	11,5	67,5	99,9	1673,65581	2,41171
•1152-01I	1,9	0,03157	0,03259	0,000847	0,5	146,7314	0,3387	5,7	73,3	99,8	1672,77707	1,33933
•1152-01J	2,1	0,04422	0,37761	0,000569	1	146,57456	0,4446	7,5	80,8	99,9	1671,61132	1,44753
•1152-01K	2,3	0,08401	0,38241	0,000359	3,2	146,61292	0,4218	7,1	87,9	99,9	1671,89653	0,89985
•1152-01L	2,6	0,02078	0,02873	0,000513	0,5	146,71478	0,7125	12,1	100	99,9	1672,65362	1,32678
Integrated age =											1658	4
(•) Plateau age =								79,7			1672	4

PFM002219A, Run ID 1153-01 (J = 0.01041 ± 0.00004):

1153-01A	1,3	0,01785	0,04622	0,007261	0	127,31957	0,5724	13,5	13,5	98,3	1522,44391	1,19021
1153-01B	1,4	0,00964	0,04481	0,000644	0,2	145,9535	0,7992	18,9	32,4	99,9	1666,98757	1,32669
1153-01C	1,4	0,01308	0,04684	0,000902	0,2	146,89116	0,4806	11,4	43,8	99,8	1673,96377	1,16258
1153-01D	1,4	0,007	0,04935	0,000058	1,6	146,98787	0,2992	7,1	50,9	100	1674,68179	1,72323
1153-01E	1,4	0,00476	0,04919	0,000144	0,4	147,15798	0,2903	6,9	57,7	100	1675,94402	1,72985
1153-01F	1,5	0,00074	0,04674	0,000371	0	147,40637	0,2136	5,1	62,8	99,9	1677,7855	2,92987
1153-01G	1,5	0,02252	0,04926	0,001819	0,2	148,08217	0,188	4,5	67,3	99,6	1682,78622	2,06797
1153-01H	1,6	0,02499	0,05101	0,001043	0,3	149,20168	0,1759	4,2	71,4	99,8	1691,03976	1,75141
1153-01I	1,6	0,03028	0,05117	0,002003	0,2	149,36676	0,1452	3,4	74,9	99,6	1692,25363	1,57978
1153-01J	1,7	0,01874	0,04749	0,000713	0,4	150,39683	0,3393	8	82,9	99,9	1699,80957	1,65739
1153-01K	1,7	0,00868	0,04753	0,000711	0,2	148,47696	0,1347	3,2	86,1	99,9	1685,70107	2,39717
1153-01L	1,8	0,03001	0,048	0,000961	0,4	149,53778	0,1099	2,6	88,7	99,8	1693,51033	2,28109
1153-01M	2	0,02944	0,04728	0,000666	0,6	149,03052	0,2368	5,6	94,3	99,9	1689,78039	1,88992
1153-01N	2,2	0,10677	0,04861	0,000321	4,5	146,96368	0,0992	2,3	96,6	99,9	1674,50221	3,21203
1153-01O	2,5	0,4402	0,04598	0,001518	3,9	146,46528	0,142	3,4	100	99,7	1670,7986	2,23297
Integrated age =											1659	4
Integrated age steps B-O											1679	4

KFM01A-100, Run ID 1158-01 (J = 0.01041 ± 0.00004):

1158-01A	1,3	0,00671	0,04456	0,003389	0	142,56688	0,9528	34,5	34,5	99,3	1641,5641	3,9371
1158-01B	1,3	0,02974	0,05128	0,001618	0,2	146,16523	0,0933	3,3	37,8	99,7	1668,5652	2,49935
•1158-01C	1,4	0,00955	0,04978	0,000615	0,2	147,70824	0,374	13,3	51,1	99,9	1680,02091	1,34495
•1158-01D	1,4	0,0083	0,05078	0,000687	0,2	147,98143	0,3351	11,9	63	99,9	1682,04164	1,24116
•1158-01E	1,5	0,01319	0,04808	0,000759	0,2	148,24778	0,3174	11,3	74,3	99,8	1684,00954	1,34467
•1158-01F	1,5	0,01857	0,0475	0,001178	0,2	148,06309	0,1689	6	80,3	99,8	1682,64516	1,8964
•1158-01G	1,6	0,03984	0,05129	0,000706	0,8	147,93906	0,1008	3,6	83,9	99,9	1681,72841	2,02841
•1158-01H	1,8	0,02236	0,05007	0,001631	0,2	147,59919	0,1587	5,6	89,5	99,7	1679,21374	2,01351
•1158-01I	2	0,03157	0,04966	0,000991	0,4	147,61775	0,1806	6,4	95,9	99,8	1679,35114	2,42317
•1158-01J	2,2	0,02312	0,05074	0,000713	0,4	147,40886	0,1141	4,1	100	99,9	1677,80398	1,89191
Integrated age =											1667	4
(•) Plateau age =								62,2			1681	4

KFM01A-1000, Run ID 1154-01 (J = 0.01041 ± 0.00004):

1154-01A	1,2	0,056	0,07286	0,006531	0,1	120,52409	0,2077	8,4	8,4	98,4	1466,70993	1,40045
1154-01B	1,3	0,0383	0,07461	0,001174	0,4	140,28242	0,2793	11,4	19,8	99,8	1624,20992	1,54012
1154-01C	1,3	0,02374	0,07345	0,000486	0,7	141,7451	0,2708	11	30,8	99,9	1635,34056	1,56626
•1154-01D	1,4	0,03012	0,07637	0,000859	0,5	142,20777	0,2925	11,9	42,7	99,8	1638,84708	2,07854
•1154-01E	1,4	0,03394	0,07351	0,000713	0,6	142,39218	0,3211	13,1	55,8	99,9	1640,2428	1,4511
•1154-01F	1,4	0,03147	0,07219	0,000332	1,3	142,60523	0,225	9,2	65	99,9	1641,85394	1,5161
•1154-01G	1,5	0,05168	0,07434	0,00016	4,4	142,22134	0,1734	7,1	72	100	1638,94983	1,90255
•1154-01H	1,5	0,06053	0,07312	0,001212	0,7	142,23349	0,1144	4,6	76,7	99,8	1639,04184	2,16896
•1154-01I	1,6	0,11142	0,07165	0,000613	2,4	142,16396	0,1059	4,3	81	99,9	1638,51537	2,65121
•1154-01J	1,8	0,34257	0,07617	0,000544	8,5	142,0316	0,1984	8,1	89,1	99,9	1637,51269	1,61098
•1154-01K	2	0,44762	0,07308	0,00061	9,9	142,04267	0,1625	6,6	95,7	99,9	1637,59656	2,11653
1154-01L	2,3	0,22255	0,07388	0,000291	10,3	141,44053	0,1054	4,3	100	99,9	1633,02848	2,0841
Integrated age=											1623	4
(•) Plateau age =								64,9			1639	4

[a] • Indicates steps included in the plateau age; Integrated age = the age calculated from all steps analysed; (•) Plateau age = the age calculated from steps that constitute a plateau, i.e. the interpreted true age of the sample

[b] Percentage of the total ^{36}Ar that are produced from Ca during irradiation (used to correct for atmospheric ^{40}Ar)

[c] Percentage ^{39}Ar released during each step

[d] Percentage of measured ^{40}Ar that is radiogenic

PFM000256A

Sample PFM000256A is a Group B, medium-grained metagranite to metagranodiorite from an outcrop to the south-west of the candidate area (Figure 1-2). The locality lies within the structural domain that shows more intense ductile deformation. The sampling locality is also situated immediately to the southwest of the Eckarfjärden deformation zone (Figure 1-2).

The plateau age defined on the $^{40}Ar/^{39}Ar$ step-heating spectrum diagram is 1671±5 Ma (Figure 5-19). The age is interpreted as the age of cooling below the closure temperature of biotite (c 300°C).

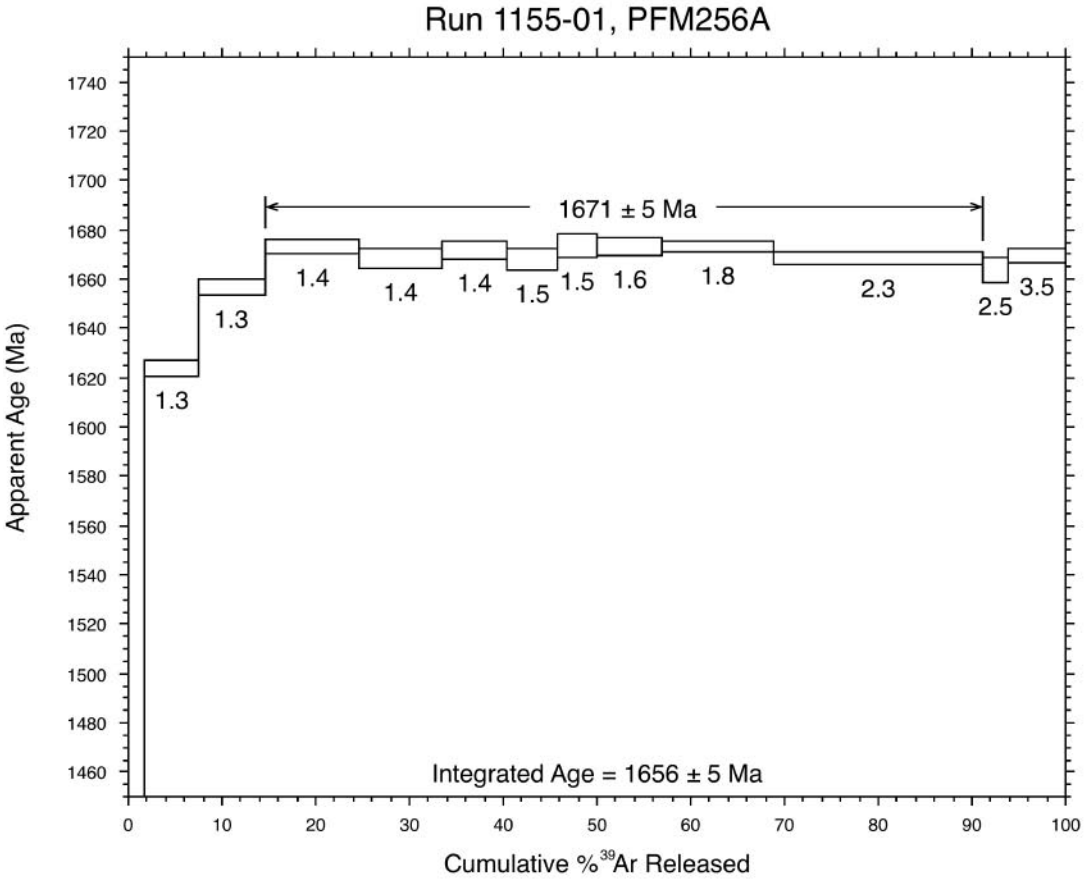

Figure 5-19. *$^{40}Ar/^{39}Ar$ biotite step-heating spectrum for sample PFM000256A.*

PFM000875A

Sample PFM000875A is a Group B metatonalite that is situated southwest of the candidate area (Figure 1-2). The locality lies within the structural domain that shows more intense ductile deformation. The sampling locality is also situated between the Eckarfjärden and Forsmark deformation zones (Figure 1-2).

The plateau age defined on the $^{40}Ar/^{39}Ar$ step-heating spectrum diagram is 1700±4 Ma (Figure 5-20). The age is interpreted as the age of cooling below the closure temperature of biotite (c 300°C).

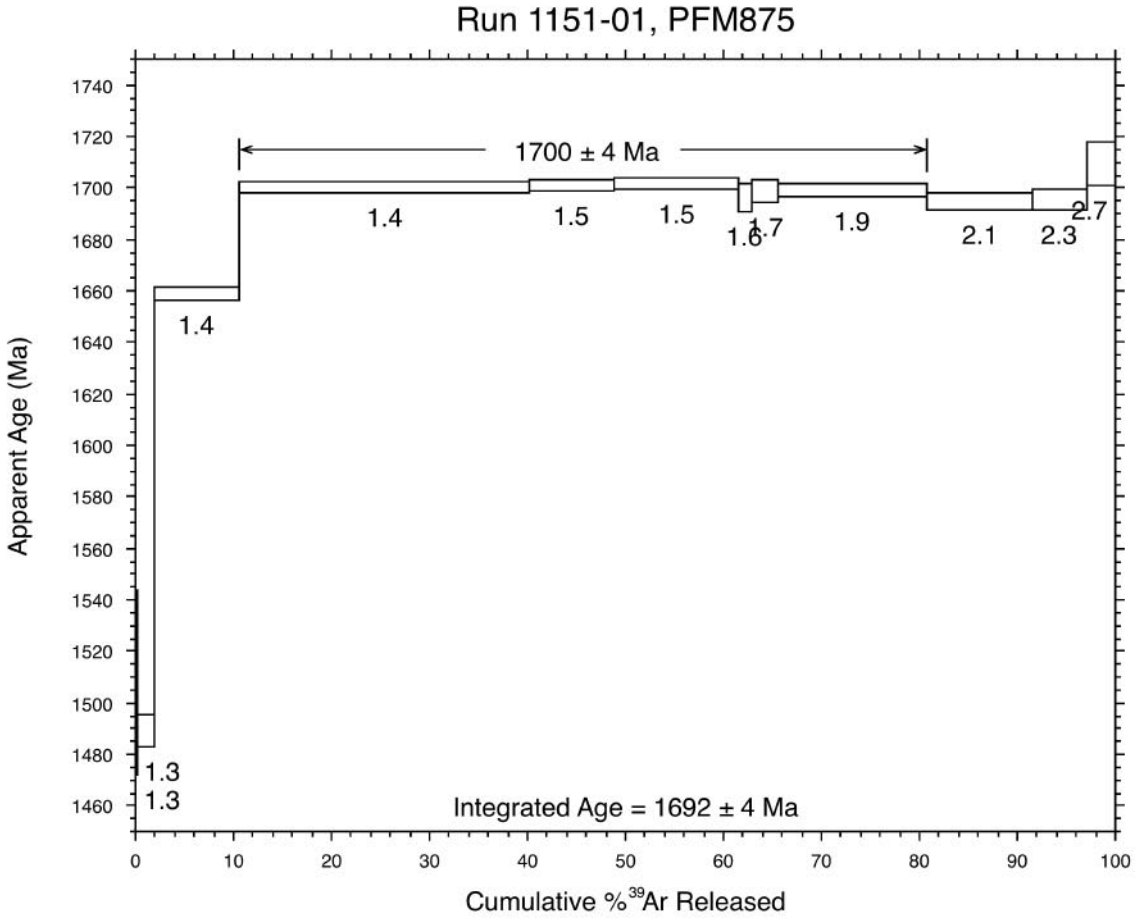

Figure 5-20. *$^{40}Ar/^{39}Ar$ biotite step-heating spectrum for sample PFM000875A.*

PFM001240A

Sample PFM001240A is a Group B metagranodiorite that is situated immediately south-west of the area selected for bedrock mapping activities (Figure 1-2). The locality lies within the structural domain that generally shows less intense ductile deformation. The sampling locality is also situated south-west of the regionally important Forsmark deformation zone (Figure 1-2).

The plateau age defined on the $^{40}Ar/^{39}Ar$ step-heating spectrum diagram is 1699±4 Ma (Figure 5-21). The age is interpreted as the age of cooling below the closure temperature of biotite (c 300°C).

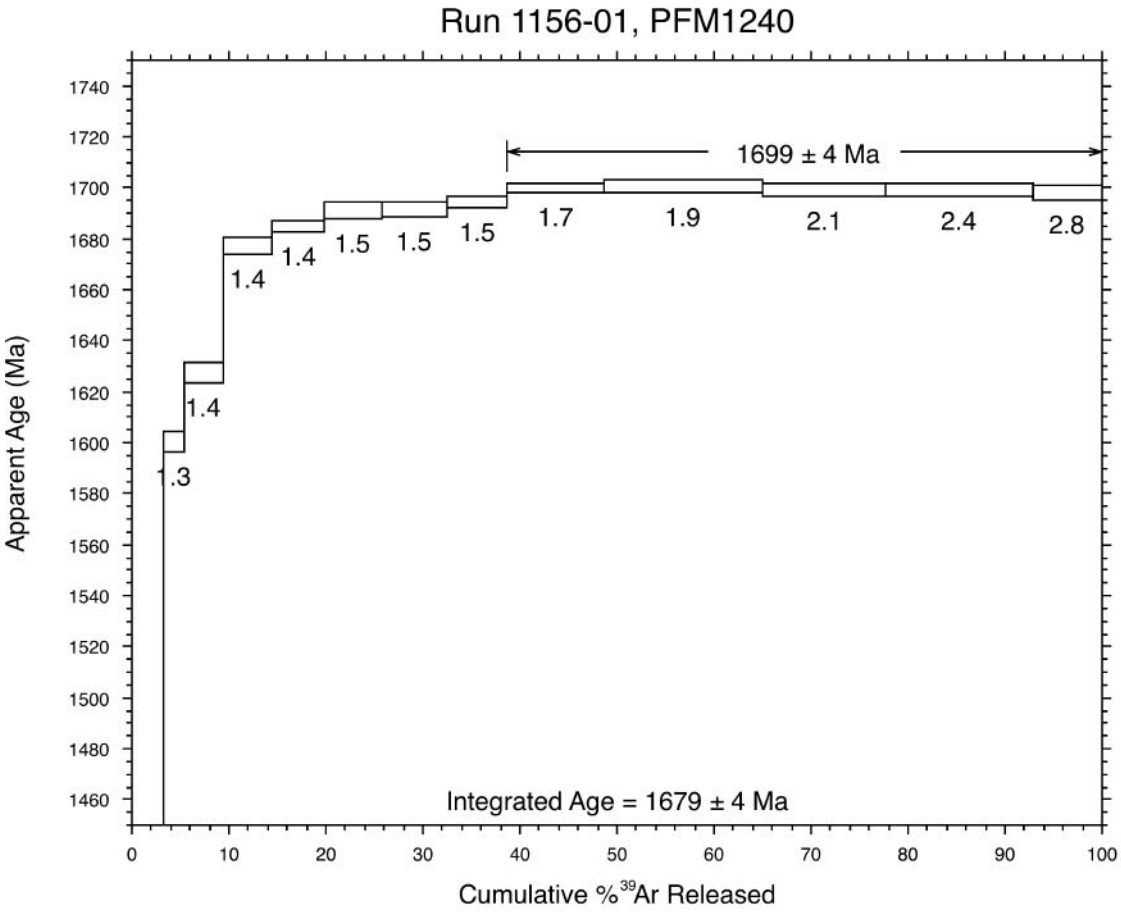

Figure 5-21. *$^{40}Ar/^{39}Ar$ biotite step-heating spectrum for sample PFM001240A.*

PFM002207A

Sample PFM002207A is a Group B, medium-grained metagranite from an outcrop inside the candidate area (Figure 1-2). The locality lies within the structural domain that generally shows less intense ductile deformation. It is also situated in the bedrock block between the Eckarfjärden and Singö deformation zones (Figure 1-2).

The plateau age defined on the $^{40}Ar/^{39}Ar$ step-heating spectrum diagram is 1680±4 Ma (Figure 5-22). The age is interpreted as the age of cooling below the closure temperature of biotite (c 300°C).

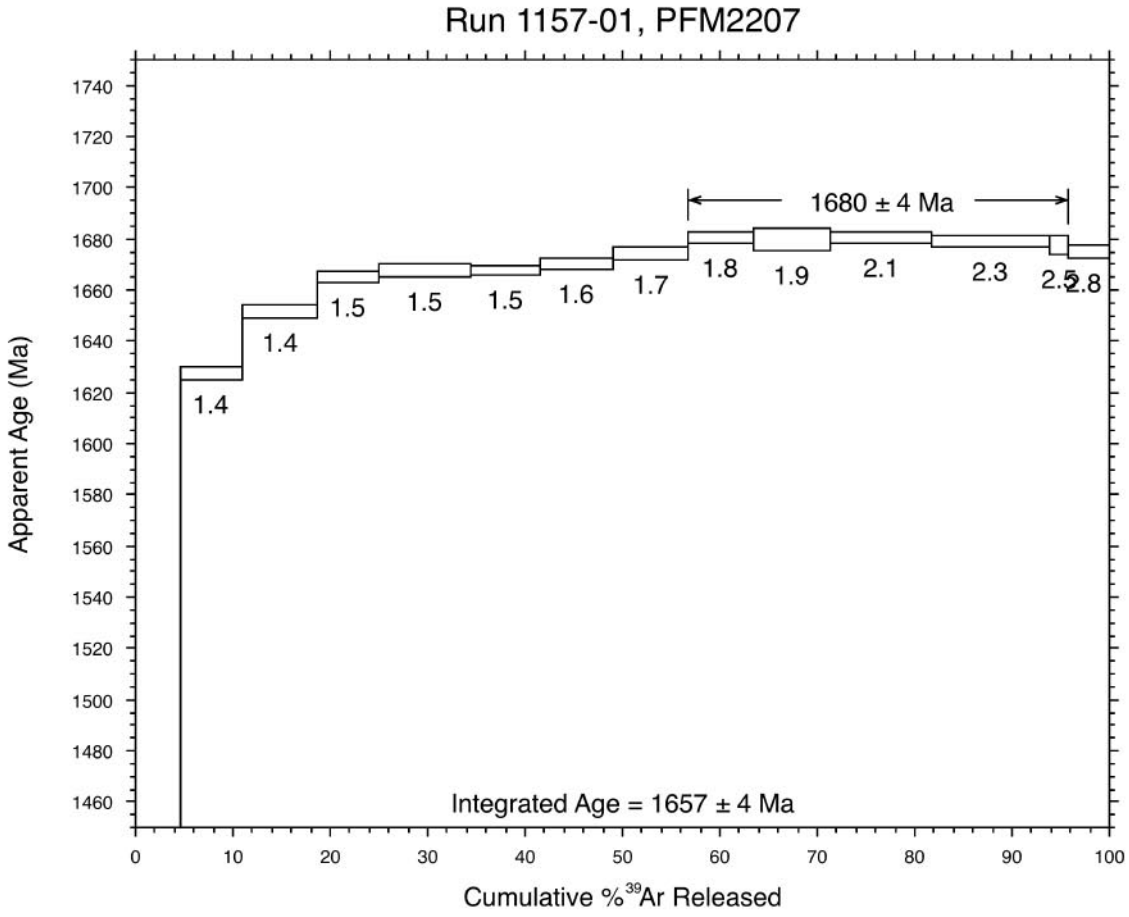

Figure 5-22. *$^{40}Ar/^{39}Ar$ biotite step-heating spectrum for sample PFM002207A.*

PFM002213A

Sample PFM002213A is a Group C metagranodiorite from a coastal outcrop on Klubbudden (Figure 1-2). The sampling locality lies within the structural domain that shows more intense ductile deformation to the north-east of the candidate area. It is also situated in the bedrock block between the Eckarfjärden and Singö deformation zones, relatively close to the Singö deformation zone (Figure 1-2).

The plateau age defined on the $^{40}Ar/^{39}Ar$ step-heating spectrum diagram is 1672±4 Ma (Figure 5-23). The age is interpreted as the age of cooling below the closure temperature of biotite (c 300°C).

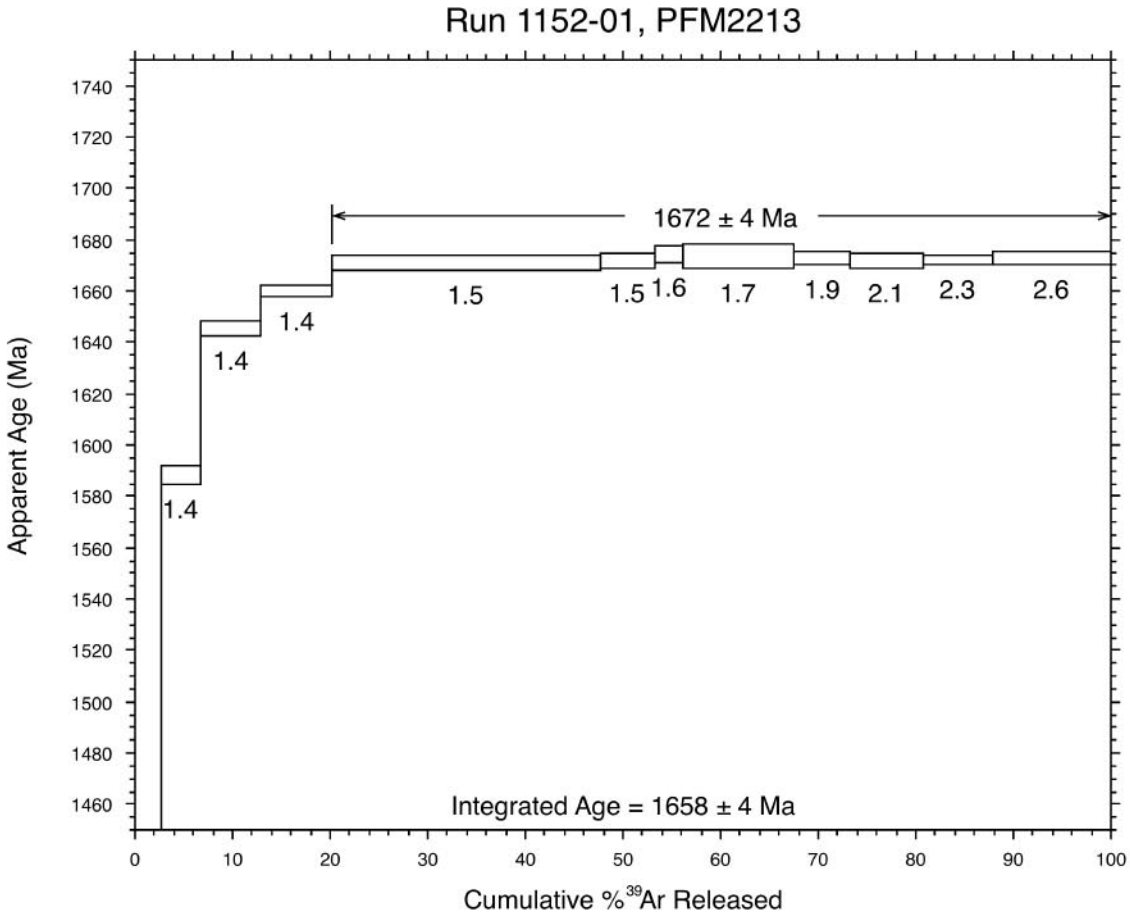

Figure 5-23. *$^{40}Ar/^{39}Ar$ biotite step-heating spectrum for sample PFM002213A.*

PFM002219A

Sample PFM002219A is a Group B, medium-grained metagranite to metagranodiorite from a small roadside outcrop close to drill site 1. This outcrop is situated inside yet close to the south-western margin of the candidate area and lies within the structural domain that generally shows less intense ductile deformation (Figure 1-2). However, the degree of ductile deformation, with the development of a distinctive, planar grain-shape fabric, increases towards the margin of the granite pluton. The sampling locality is also situated in the bedrock block between the Eckarfjärden and Singö deformation zones (Figure 1-2).

Sample PFM002219A did not yield a well-constrained plateau age (Figure 5-24). However, an integrated age from steps B to O, which accounts for 86.5% of the gas released (Table 5-4), is 1679±4 Ma. This age coincides with the other $^{40}Ar/^{39}Ar$ biotite ages obtained from samples within the candidate area. For this reason, this age is interpreted as the age of cooling below the closure temperature of biotite (c 300°C).

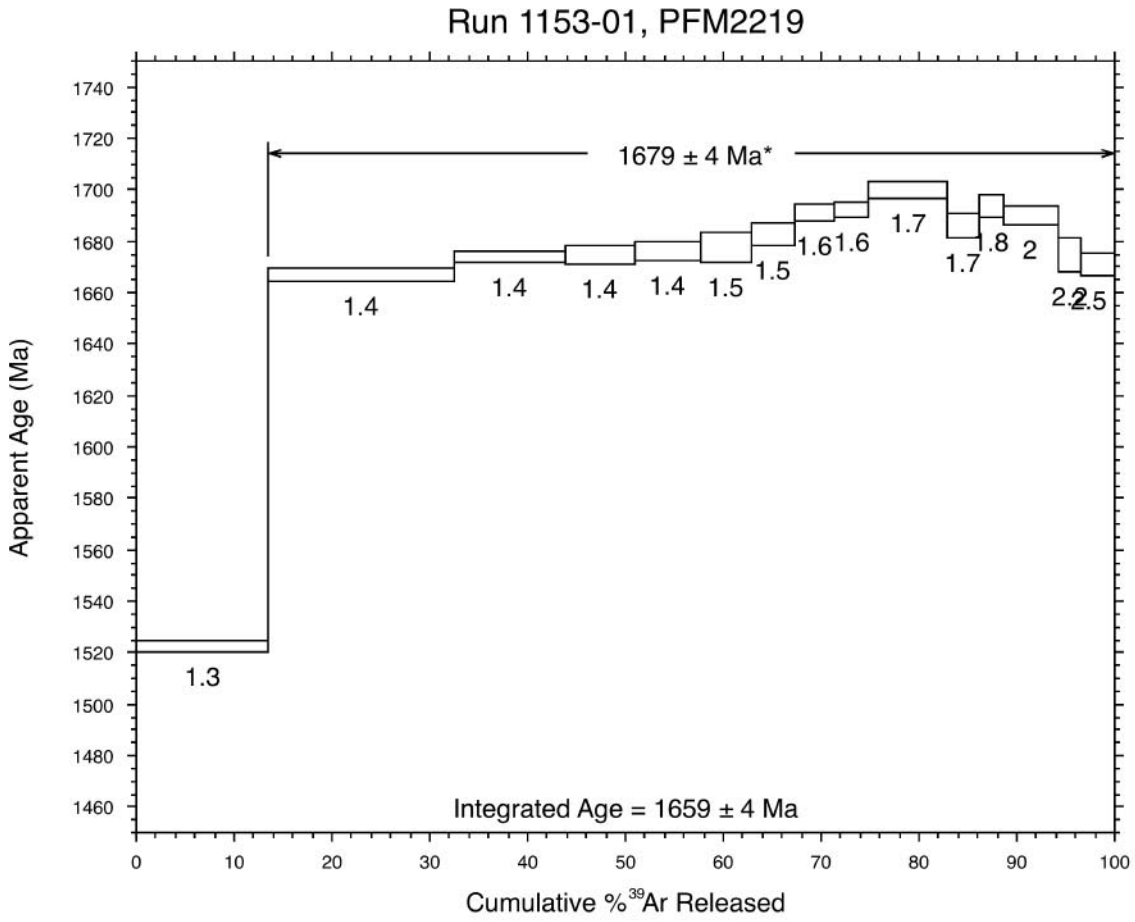

Figure 5-24. *$^{40}Ar/^{39}Ar$ biotite step-heating spectrum for sample PFM002219A. The asterisk indicates that there is no true plateau according to the criteria used here /Dalrymple and Lanphere, 1971/.*

KFM01A-100

Sample KFM01A-100 is a Group B, medium-grained metagranite to metagranodiorite that was sampled in the 108.5–108.9 m depth interval in borehole KFM01A. This borehole intersects the bedrock within the structural domain that generally shows less intense ductile deformation (Figure 1-2). However, the degree of ductile deformation, with the development of a distinctive, planar grain-shape fabric, increases towards the margin of the granite pluton where KFM01A is situated. Borehole KFM01A also intersects the bedrock block between the Eckarfjärden and Singö deformation zones (Figure 1-2).

The $^{40}Ar/^{39}Ar$ step-heating plateau age is 1681±4 Ma (Figure 5-25). The age is interpreted as the age of cooling below the closure temperature of biotite (c 300°C).

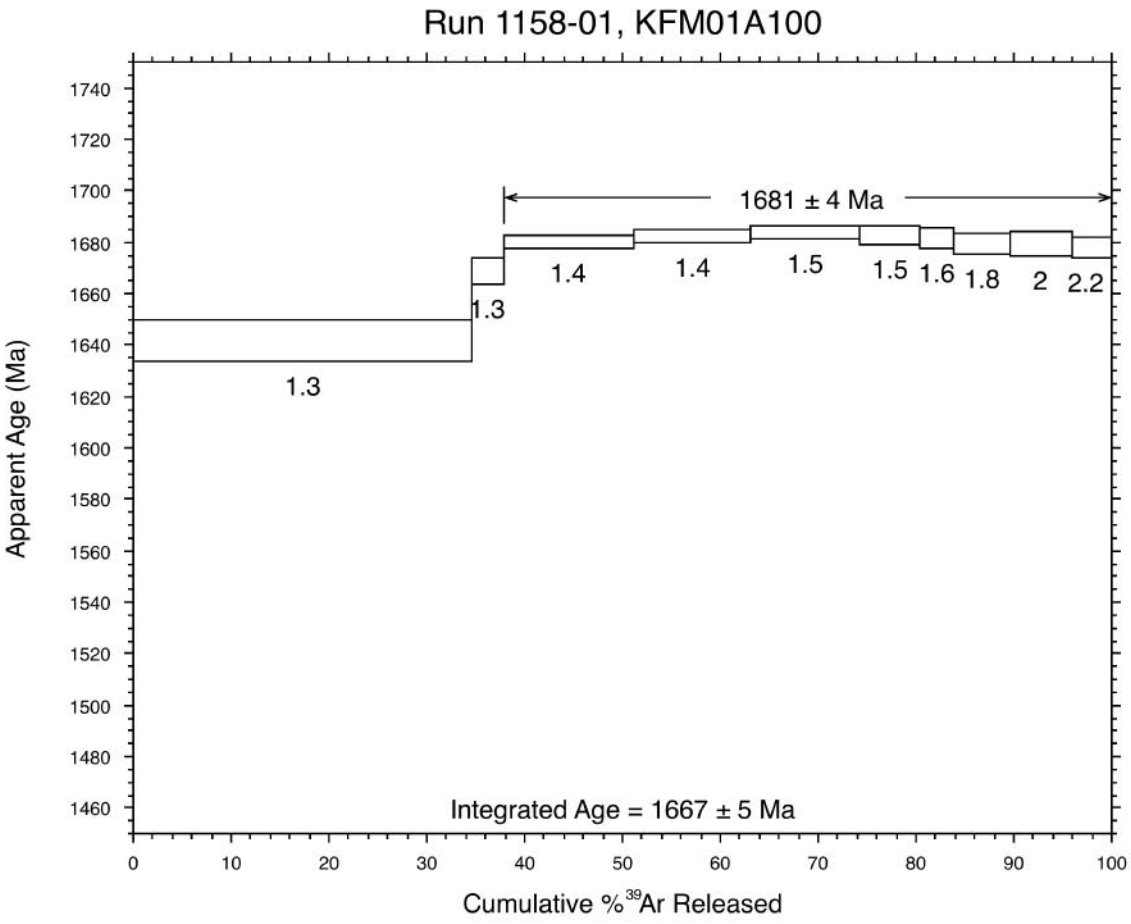

Figure 5-25. *$^{40}Ar/^{39}Ar$ biotite step-heating spectrum for sample KFM01A-100.*

KFM01A-1000

Sample KFM01A-100 is a Group B, medium-grained metagranite to metagranodiorite that was sampled in the 1001.2–1001.6 m depth interval in borehole KFM01A. This borehole intersects the bedrock within the structural domain that generally shows less intense ductile deformation (Figure 1-2). However, the degree of ductile deformation, with the development of a distinctive, planar grain-shape fabric, increases towards the margin of the granite pluton where KFM01A is situated. Borehole KFM01A also intersects the bedrock block between the Eckarfjärden and Singö deformation zones (Figure 1-2).

The $^{40}Ar/^{39}Ar$ step-heating plateau age is 1639±4 Ma (Figure 5-26). The age is interpreted as the age of cooling below the closure temperature of biotite (c 300°C).

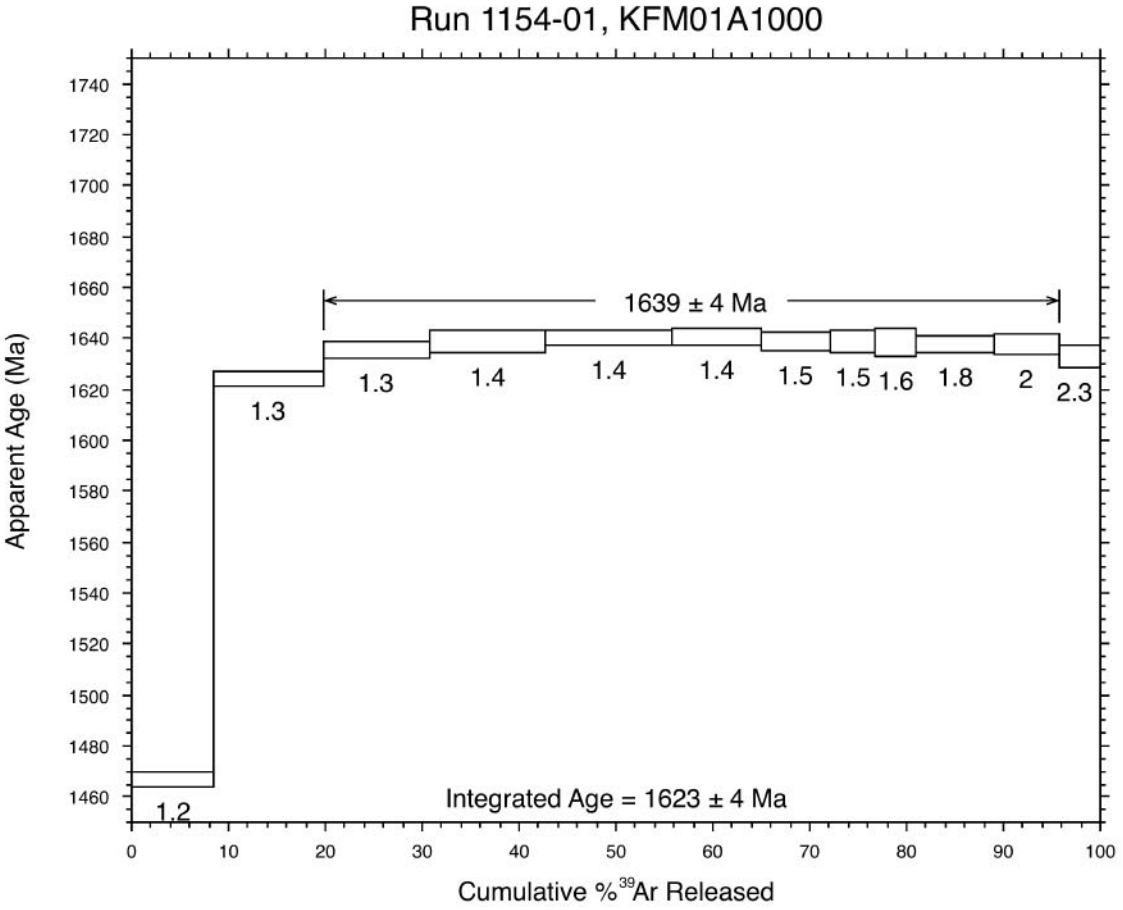

Figure 5-26. *$^{40}Ar/^{39}Ar$ biotite step-heating spectrum for sample KFM01A-1000.*

5.4 (U-Th)/He ages

When apatite crystallises, U and Th are incorporated into the crystal lattice. Both isotopes subsequently decay with emission of alpha particles (= ^{4}He nuclei). Helium is completely mobile in apatite down to a temperature of c 70–60°C /Farley, 2000/, after which it starts to be retained in the crystal. However, helium diffusion continues at lower temperatures, though at progressively slower rates, until complete retention occurs below c 40°C. This temperature range is referred to as the *He*lium *P*artial *R*etention *Z*one (HePRZ) and is analogous to the *P*artial *A*nnealing *Z*one (PAZ) used in apatite fission-track thermochronology /Gallagher et al, 1998/. Due to its sensitivity at low temperatures, the (U-Th)/He method has been used in interdisciplinary fields within geomorphology, landform evolution, structural geology and geodynamics.

The (U-Th)/He data that have been used to calculate the ages presented in this report are listed in Table 5-5. These include age determinations from two surface samples, on opposite sides of the Eckarfjärden deformation zone (Figure 1-2), and from five samples from different depths (c 200, 400, 600, 800 and 1000 m) in KFM01A (Figure 1-2).

Table 5-5. (U-Th)/He data.

Sample[a]	^{238}U (ppm)	^{235}U (ppm)	Th (ppm)	He cm^3/g	Ft[b]	Raw age (Ma)	Corr. Age (Ma)	Error (± 2σ)
PFM000875Ap1	10,918	0,079	1,181	4,44E-04	0,648	326	503,4	19,9
PFM002219Ap1	9,745	0,071	3,684	4,99E-04	0,611	386	632,8	22,3
PFM002219Ap2	11,612	0,084	3,686	6,22E-04	0,695	410	590,4	23,9
KFM01A-200p1	9,075	0,066	4,677	3,79E-04	0,733	307	418,5	17,2
KFM01A-200p2	11,975	0,087	5,608	6,51E-04	0,785	403	513,4	22,8
KFM01A-400p1	5,816	0,042	3,080	2,42E-04	0,668	304	454,7	17,0
KFM01A-400p2	6,313	0,046	3,057	1,87E-04	0,594	219	368,9	12,4
KFM01A-600p1	8,826	0,064	8,029	2,61E-04	0,726	200	275,8	10,6
KFM01A-600p2	6,442	0,047	5,246	2,14E-04	0,699	229	327,6	12,3
KFM01A-800p1	7,444	0,054	4,527	1,81E-04	0,611	175	286,5	9,7
KFM01A-1000p1	13,320	0,097	11,120	3,01E-04	0,619	155	251,2	8,3
KFM01A-1000p2	20,928	0,152	16,014	4,87E-04	0,567	159	281,2	8,6

[a]p1 and p2 at the end of the sample names refers to splits of same sample
[b]Ft = alpha-ejection correction factor

The age obtained from the metatonalite within the bedrock block between the Forsmark and Eckarfjärden deformation zones (Figure 1-2) is c 100 Ma younger than the age obtained from the medium-grained metagranite in the bedrock block to the north-east, between the Eckarfjärden and Singö deformation zones (Figure 1-2). This age difference exists even after account is taken of the analytical errors involved. More data are required to investigate the geological significance of this result.

The data from KFM01A indicate consistently younger ages with depth (Figure 5-27), ranging from c 630 Ma from the surface sample close to drill site 1 (PFM002219A) down to c 250 Ma at the bottom of borehole KFM01A (c 1000 m). However, a change in slope on the age–depth diagram can be observed at a depth of c 600 m (Figure 5-27).

Age–depth correlations possibly reveal the lower part of a fossil HePRZ in the upper part of the diagram. The steeper slope on the diagram beneath this possible HePRZ represents an exhumation event that had to occur to preserve the zone. From this set of data, the age of the onset of this event can be estimated to a minimum of c 300 Ma. The exhumation rate, defined by a regression line through the steeper part between the ages of c 300 Ma and c 250 Ma, is c 4 m/Ma. For comparison purposes, it may be noted that the present rate of uplift in northern Uppland, following the latest glaciation, is 6000 m/Ma. More samples from KFM01A as well as other boreholes will be analysed at a later stage, in order to provide tighter constraints on the age and character of the exhumation event.

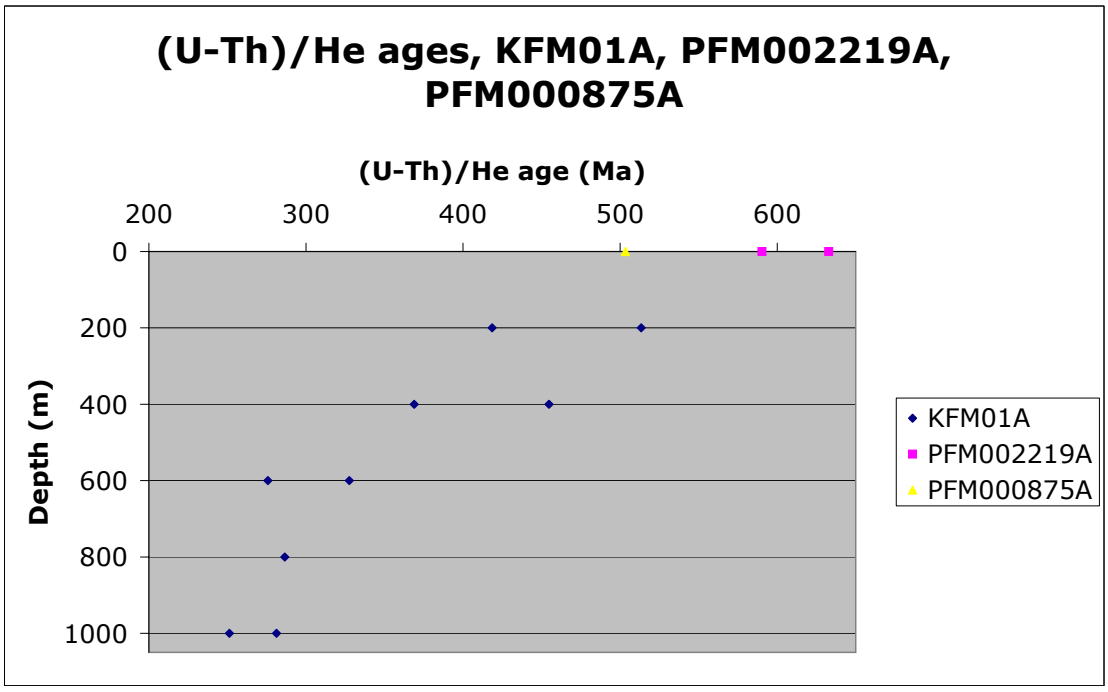

Figure 5-27. *(U-Th)/He ages plotted on an age–depth diagram. The spread in the duplicates are likely due to grain-size differences. The lower part of the slope, between 600 m and 1000 m, may represent an exhumation event that is estimated to have started at a minimum age of c 300 Ma.*

6 Conclusions

A summary of the geological features at the Forsmark site upon which the age-dating work has been focused and the ages obtained are presented in Tables 6-1 and 6-2.

Table 6-1. Ages of crystallisation of the igneous rocks at the Forsmark site.

Age of crystallisation of igneous rocks			
Geological feature	**Dated rock type**	**Method**	**Age**
Supracrustal rocks (Group A)	−	−	*Comment:* Age inferred to be older than 1885 Ma.
Older calc-alkaline plutons with ultramafic to intermediate, tonalitic and granodioritic compositions (Group B intrusive rocks)	1. Metagabbro 2. Metatonalite to metagranodiorite	1. U-Pb zircon (TIMS) 2. U-Pb zircon (SIMS)	1. 1886±0.9 Ma 2. 1883±3.4 Ma
Older calc-alkaline plutons with granitic to granodioritic composition (Group B intrusive rocks)	Metagranite inside the candidate area	U-Pb zircon (SIMS)	1865±3.4 Ma
Mafic dyke-like bodies and irregular minor intrusions in Group B metagranite to metagranodiorite	−	−	*Comment:* Field relationships indicate similar or younger age relative to the Group B metagranite to metagranodiorite. Age of cooling through the 700–550°C temperature interval is 1843±3 Ma (see below). Age of intrusion inferred to be 1868–1840 Ma.
Younger, calc-alkaline, dyke-like bodies and minor intrusions with granodioritic to tonalitic composition (Group C intrusive rocks)	Metagranodiorite	U-Pb zircon (SIMS)	1864±3.4 Ma
Younger calc-alkaline dykes and intrusions with granitic composition (included in Group D intrusive rocks)	Granite	U-Pb zircon (SIMS)	1851±5.2 Ma *Comment:* The age is supported by the U-Pb titanite age (see below) from the same rock type.

Table 6-2. Timing of ductile deformation as well as cooling and exhumation ages at the Forsmark site.

Timing of ductile deformation. Cooling and exhumation ages			
Geological feature	**Dated rock type**	**Method**	**Age**
Penetrative ductile deformation under amphibolite-facies metamorphic conditions	−	−	*Comment:* Field relationships indicate that penetrative deformation in the coastal area (Klubbudden) affected the Group B rocks and was complete prior to intrusion of the group D dykes*, i.e. is constrained to the time interval 1868−1846 Ma.* The intense tectonic banding in this area affected the Group B rocks and was established prior to intrusion of the Group C rocks, *i.e.developed around 1865 Ma.*
Discrete ductile deformation under lower amphibolite- or greenschist-facies metamorphic conditions	−	−	*Comment:* Field relationships indicate that this type of deformation affects the Group D rocks, *i.e. developed after 1856 Ma.*
Cooling below 700–550°C	1. Group B amphibolite	U-Pb titanite (TIMS)	1. 1843±3 Ma
	2. Group D granite		2. 1844±4 Ma
Cooling below c 500°C	Group B amphibolite (eight samples) and metagabbro (one sample)	$^{40}Ar/^{39}Ar$ hornblende	1834−1793 Ma *Comment:* Variation in age in different structural domains.
Cooling below c 300°C	Various Group B and Group C felsic meta-intrusive rocks (eight samples)	$^{40}Ar/^{39}Ar$ biotite	1704−1635 Ma *Comment:* Variation in age at the surface in different bedrock blocks and a younger age with depth in KFM01A. Age difference between the samples in KFM01A suggests an uplift rate of c 25 m/Ma.
Cooling below c 70–60°C	Group B metagranite to metagranodiorite, predominantly from KFM01A (seven samples)	(U-Th)/He	c 630−250 Ma *Comment:* (U-Th)/He ages are younger with depth in KFM01A, with a possible exhumation event between c 300 and 250 Ma. Borehole data indicate an uplift rate of c 4 m/Ma. Variation also at the surface in different bedrock blocks.

The present data indicate that there are systematic spatial variations in $^{40}Ar/^{39}Ar$ (hornblende, biotite) and (U-Th)/He ages, both at the surface in different ductile structural domains ($^{40}Ar/^{39}Ar$ hornblende) and in different bedrock blocks ($^{40}Ar/^{39}Ar$ biotite and (U-Th)/He), and at depth along borehole KFM01A. More data from both surface and borehole samples are required to understand better the important geological implications of these spatial variations.

7 References

Bergman T, Andersson J, Hermansson T, Petersson J, Zetterström Evins L, Nordman C, Albrecht L, Stephens M B, 2004. Forsmark site investigation. Bedrock mapping. Stage 2 (2003) – Bedrock data from outcrops and the basal parts of trenches and shallow boreholes through the Quaternary cover. SKB P-04-91, Svensk Kärnbränslehantering AB.

Corfu F, in press. U-Pb age, setting and tectonic significance of the anorthosite-mangerite-charnockite-granite-suite, Lofoten-Vesterålen, Norway. Journal of Petrology.

Corfu F, Andersen T B, 2002. U-Pb ages of the Dalsfjord Complex, SW Norway, and their bearing on the correlation of allochthonous crystalline segments of the Scandinavian Caledonides. International Journal of Earth Sciences 91, 955–963.

Dalrymple G B, Lanphere M A, 1971. $^{40}Ar/^{39}Ar$ technique of K-Ar dating: a comparison with the conventional technique. Earth and Planetary Science Letters 12, 300–308.

Davis D W, Blackburn C E, Krogh T E, 1982. Zircon U-Pb ages from the Wabigoon-Manitou Lakes region, Wabigoon Subprovince, northwest Ontario. Canadian Journal of Earth Sciences 19, 254–266.

Farley K A, 2000. Helium diffusion from apatite: general behaviour as illustrated by Durango flourapatite. Journal of Geophysical Research 105, 2903–2914.

Frost B R, Chamberlain K R, Schumacher J C, 2000. Sphene (titanite): phase relations and role as a geochronometer. Chemical Geology 172, 131–148.

Gallagher K, Brown R, Christopher J, 1998. Fission-track analysis and its applications to geological problems. Annual Revue of Earth and Planetary Sciences 26, 519–572.

Isaksson H, 2003. Forsmark site investigation. Interpretation of topographic lineaments 2002. SKB P-03-40, Svensk Kärnbränslehantering AB.

Isaksson H, Mattsson H, Thunehed H, Keisu M, 2004a. Forsmark site investigation. Interpretation of petrophysical surface data. Stage 1 (2002). SKB P-03-102, Svensk Kärnbränslehantering AB.

Isaksson H, Thunehed H, Keisu M, 2004b. Forsmark site investigation. Interpretation of airborne geophysics and integration with topography. Stage 1 (2002). SKB P-04-29, Svensk Kärnbränslehantering AB.

Jonckheerre R, Mars M, Van den Haute P, Rebetez M, Chambaudet A, 1993. L'apatite de Durango (Mexique): analyse d'un mineral standard pour la datation par traces de fission. Chemical Geology 103, 141–154

Krogh T E, 1973. A low contamination method for hydrothermal decomposition of zircon and extraction of U and Pb for isotopic age determinations. Geochimica et Cosmochimica Acta 37, 485–494.

Krogh T E, 1982. Improved accuracy of U-Pb zircon ages by the creation of more concordant systems using an air abrasion technique. Geochimica et Cosmochimica Acta 46, 637–649.

Ludwig K R, 2003. A geochronological toolkit for Microsoft Excel, Berkeley Geochronological Center, Special Publication No. 4, 75 pp.

Mattsson H, Isaksson H, Thunehed H, 2003. Forsmark site investigation. Petrophysical rock sampling, measurements of petrophysical rock parameters and in situ gamma-ray spectrometry measurements on outcrops carried out 2002. SKB P-03-26, Svensk Kärnbränslehantering AB.

Renne P R, Swisher C C, Deino A L, Karner D B, Owena T L, DePaolo D J, 1998 Intercalibration of standards, absolute ages and uncertainties in $^{40}Ar/^{39}Ar$ dating. Chemical Geology 145, 117–152.

Stacey J S, Kramers J D, 1975. Approximation of terrestrial lead isotope evolution by a two-stage model. Earth and Planetary Science Letters 26, 207–221.

Stephens M B, Bergman T, Andersson J, Hermansson T, Wahlgren C-H, Albrecht L, Mikko H, 2003a. Forsmark. Bedrock mapping. Stage 1 (2002) − Outcrop data including fracture data. SKB P-03-09, Svensk Kärnbränslehantering AB.

Stephens M B, Lundqvist S, Bergman T, Andersson J, 2003b. Forsmark site investigation. Bedrock mapping. Rock types, their petrographic and geochemical characteristics, and a structural analysis of the bedrock based on Stage 1 (2002) surface data. SKB P-03-75, Svensk Kärnbränslehantering AB.

Whitehouse M J, Claesson S, Sunde T, Vestin J, 1997. Ion microprobe U-Pb zircon geochronology and correlation of Archaean gneisses from the Lewisian Complex of Gruinard Bay, northwestern Scotland. Geochimica et Cosmochimica Acta 61, 4429–4438.

Whitehouse M J, Kamber B S, Moorbath S, 1999. Age significance of U-Th-Pb zircon data from early Archaean rocks of west Greenland – a reassessment based on combined ion-microprobe and imaging studies. Chemical Geology 160, 201–224.

Wiedenbeck M, Allé P, Corfu F, Griffin W L, Meier M, Oberli F, von Quadt A, Roddick J C, Spiegel W, 1995. Three natural zircon standards for U-Th-Pb, Lu-Hf, trace element and REE analysis. Geostandards Newsletter 19, 1–23.

Wijbrans J R, Pringle M S, Koppers A A P, Scheveers R, 1995. Argon geochronology of small samples using the Vulkaan argon laserprobe. Proceedings of the Koninklijke Nederlandse akademie van wetenschappen 98, 185–218.